Submitted to NUCLEAR PHYSICS B

LBL-7745
Preprint c.2

QUANTUM CHROMODYNAMICS AT HIGH TEMPERATURE

Joseph I. Kapusta

June 1978

Prepared for the U. S. Department of Energy
under Contract W-7405-ENG-48

RECEIVED
LAWRENCE
BERKELEY LABORATORY

SEP 12 1978

LIBRARY AND
DOCUMENTS SECTION

TWO-WEEK LOAN COPY

This is a Library Circulating Copy which may be borrowed for two weeks. For a personal retention copy, call Tech. Info. Division, Ext. 6782

LBL-7745 c.2

DISCLAIMER

This document was prepared as an account of work sponsored by the United States Government. While this document is believed to contain correct information, neither the United States Government nor any agency thereof, nor the Regents of the University of California, nor any of their employees, makes any warranty, express or implied, or assumes any legal responsibility for the accuracy, completeness, or usefulness of any information, apparatus, product, or process disclosed, or represents that its use would not infringe privately owned rights. Reference herein to any specific commercial product, process, or service by its trade name, trademark, manufacturer, or otherwise, does not necessarily constitute or imply its endorsement, recommendation, or favoring by the United States Government or any agency thereof, or the Regents of the University of California. The views and opinions of authors expressed herein do not necessarily state or reflect those of the United States Government or any agency thereof or the Regents of the University of California.

LBL-7745

QUANTUM CHROMODYNAMICS AT HIGH TEMPERATURE

Joseph I. Kapusta

Lawrence Berkeley Laboratory
University of California
Berkeley, California 94720

ABSTRACT

The thermodynamic potential of quantum chromodynamics is calculated in orders 1, α_c and $\alpha_c^{3/2}$. The renormalization group is used to improve the expansion by allowing α_c to be a function of the temperature and chemical potentials. The results are valid for an arbitrary number of quark flavors and masses. Numerical calculations are made for the special case of up, down and strange quarks. Particular attention is paid to the breakdown of the perturbation expansion, and possible connection to the thermodynamics of Hagedorn is discussed. The MIT bag model, which has a fixed coupling constant, does not appear to yield good convergence at high temperatures.

1. INTRODUCTION

In the last few years there has been a surge of interest in relativistic many-body systems. This has largely been due to progress in elementary particle physics, in which gauge theories of the strong, electromagnetic and weak interactions have come to prominence. From renormalization group arguments and experiment it is known that the electromagnetic and weak interactions have a coupling constant that is small except for energies approaching those of cosmological magnitude. Furthermore, the standard gauge theory of the strong interactions, quantum chromodynamics, has a coupling constant which is large at low energy but becomes small at energies of the order of several proton masses. [For a review see Ref. 1.] As opposed to standard strong interaction field theories, where the fields are associated with ordinary hadrons and consequently large coupling constants, it is reasonable to expect that a perturbative expansion of thermodyanmic quantities converges at high densities and temperatures. At present perturbation theory is the only "reliable" calculational tool in relativistic quantum field theories.

Recent papers have concentrated on several important problems. It has been shown[2,3] that above a certain critical temperature there is a restoration of the spontaneously broken gauge symmetry of the weak interactions. Based on the renormalization group result that the strong interaction coupling in QCD goes to zero at asymptotically high energy, it was suggested that at very high densities hadronic matter was describable as a gas of free quarks.[4] Subsequent investigation[5-9] was made into the ground state properties of a quark gas to second order in

the coupling using the phenomenological MIT bag model of confinement[10,11] and/or a density dependent coupling. The proper quantization and renormalization of many-body gauge theories has been extensively discussed,[12-16] and calculations for the ground state energy of a quark gas have been carried out to fourth order in the zero mass limit[14,16] and in the nonrelativistic limit.[17]

Missing so far is an explicit calculation at finite temperature. In this paper we calculate the thermodynamic potential of quantum chromodynamics at finite temperature for an arbitrary number of fermions with arbitrary masses and chemical potentials. The calculation is explicit in orders two and three, and an outline is given of the fourth order. A calculation in fourth order for finite temperature and finite masses will involve considerably more work than at zero temperature and zero mass.

Many of the diagrams in QCD are similar to those in QED. The second and third order calculations at finite temperature for that theory have already been done.[18] Our calculations agree with those.

In Section 2 we give a brief review of the finite temperature and chemical potential Feynman rules for unbroken gauge theories. We also fix the metric and some notational conventions.

The thermodynamic potential for QCD is evaluated at the second order in Section 3 and at the third order in Section 4. Section 5 gives an outline of the calculation at fourth order.

Section 6 contains a summary of the relevant aspects of the renormalization group. In particular the effect of finite fermion masses is considered, and the choice of a convenient subtraction energy is made.

In Section 7 we examine some physical consequences of these calculations. The breakdown of perturbation theory with the possibility of a phase transition is investigated, and an estimate is made of the temperature and chemical potential dependence of this transition point. Comparisons are made among QCD with a temperature and chemical potential dependent coupling, the MIT bag model with a constant coupling and bag pressure, and the Hagedorn statistical bootstrap model of high temperature matter.[19]

We make some tentative conclusions and mention possibilities for further research in Section 8.

2. PERTURBATIVE EXPANSION OF THE THERMODYNAMIC POTENTIAL

In this section we give a brief summary of the Feynman rules for calculating the thermodynamic potential of gauge theories at arbitrary temperature and chemical potential. Their derivation may be found in several recent papers.[12,14,16]

We use units such that $\hbar = c = k$ (Boltzmann's constant) $= 1$. The Minkowski metric with $g^{oo} = -g^{ii} = 1$ is used consistently throughout the paper. There is no advantage in switching to a Euclidean metric when doing calculations at finite temperature, as opposed to the zero temperature limit.

In ordinary (nongauge) many-body theory one starts with the partition function $\mathrm{Tr}\,\exp[-\beta(H - \underset{\sim}{\mu} \cdot \underset{\sim}{N})]$ from which all thermodynamic quantities can be calculated. Here β is the inverse temperature, H the Hamiltonian and $\underset{\sim}{N}$ the conserved quantum numbers of the system with their associated chemical potentials $\underset{\sim}{\mu}$. In gauge theories it is known that $\mathrm{Tr}\,\exp[-\beta(H-\underset{\sim}{\mu}\cdot\underset{\sim}{N})]$ is in general a gauge-dependent quantity. The reason is that specious degrees of freedom will appear in H if we use a nonphysical gauge. The trace over H will include these specious particles and so will not be physically meaningful. Of course no problems arise if one always works in physical gauges, but calculations are usually simplified if a Lorentz and gauge covarient computational scheme can be found.

Such a computational scheme, suggested by Bernard,[12] is based on Feynman's path-integral formulation of statistical mechanics.[20,21] The partition function is represented as a functional integral over all fields ϕ weighted by the exponential of an effective action:

$$Z = N(\beta) \int_{\substack{\text{periodic boson} \\ \text{antiperiodic fermion}}} [d\phi] \exp\left\{ i \int_0^{-i\beta} dx_0 \int_V d^3x \, \mathcal{L}_{eff}(\phi(x), \partial_\mu \phi(x); \underset{\sim}{\mu}) \right\} . \tag{2.1}$$

Here $N(\beta)$ is a normalization factor. In quantum chromodynamics Faddeev-Popov ghost fields appear.[22,23] These ghosts are unphysical spin-zero particles which have a fermion-like minus sign for loops. Ghosts appear in order to cancel the effects of working in unphysical gauges.

$$\mathcal{L}_{eff} = \bar{\psi}(i\not{\partial} - m - g \not{A}^a \tau_a + \mu\gamma^0)\psi + (\partial_\mu \bar{\omega})(\partial^\mu \omega) + g f^{abc} \bar{\omega}_a \partial_\mu A^\mu_c \omega_b$$
$$- \frac{1}{4} F^{\mu\nu}_a F^a_{\mu\nu} - \frac{1}{2\alpha} (\partial_\mu A^\mu_a)^2 , \tag{2.2}$$

where

$$F^{\mu\nu}_a = \partial^\mu A^\nu_a - \partial^\nu A^\mu_a - g f_{abc} A^\mu_b A^\nu_c . \tag{2.3}$$

α is the gauge-fixing parameter. ψ, A and ω are respectively the fermion, gluon and ghost fields. The τ matrices are generators of the color gauge group and the f_{abc} are the structure constants :

$$[\tau^a, \tau^b] = i f^{abc} \tau_c . \tag{2.4}$$

The thermodynamic potential Ω is defined as

$$\beta V \Omega = -\log Z . \tag{2.5}$$

The part due to interactions may be isolated by writing

$$\beta V \Omega_I = \beta V(\Omega - \Omega_0) = -\log \frac{\int [d\phi] \exp\left\{ i \int_0^{-i\beta} dx_0 \int_V d^3x \, \mathcal{L}_{eff} \right\}}{\int [d\phi] \exp\left\{ i \int_0^{-i\beta} dx_0 \int_V d^3x \, \mathcal{L}^0_{eff} \right\}} , \tag{2.6}$$

where Ω_0 and $\mathcal{L}^0_{eff}$ are the thermodynamic potential and effective Lagrangian in the absence of interactions, i.e. with the coupling constant set to zero. As discussed by several authors[12,14,16] this formula for Ω_I is completely gauge-independent, i.e. independent of what value of α we choose. However, the way this works in practice can be rather subtle. It turns out that, in general, the coupling constant g is a gauge-dependent quantity. Hence it is the quantity

$$\frac{d}{d\alpha}\,\Omega_I\big(g(\alpha),\alpha\big) = \left[\frac{\partial}{\partial\alpha} + \frac{\partial g}{\partial\alpha}\,\frac{\partial}{\partial g}\right]\Omega_I\big(g(\alpha),\alpha\big)$$

which vanishes and not $(\partial/\partial\alpha)\Omega_I$. Furthermore, as discussed in Section 6, if the renoramlization group is used to improve a perturbative expansion in powers of g then α is not a fixed quantity but varies with the subtraction energy as does g. The exception is the Landau gauge in which α is always zero.

One can do a straightforward diagramatic expansion for Ω_I in powers of the coupling constant in the usual way.[14] This expansion may be in terms of bare propagators and vertices. Alternatively one may perform a Legendre transformation and do an expansion in terms of full propagators and vertices. The lower order diagrams will be considered in Sections 3-5.

The bare propagators and vertices for quantum chromodynamics are shown in Fig. 1. The conventions for factors of -1 and i are chosen to be compatible with the diagrams of Freedman and McLerran.[14] The three-momenta $\underset{\sim}{p}$ are continuous and there is a three-momenta conserving Dirac delta at each vertex: $(2\pi)^3\delta^3(\underset{\sim}{p}_{in}-\underset{\sim}{p}_{out})$. The zero components of the momenta, p^0, are $2\pi niT$ for bosons and $(2n+1)\pi iT+u$ for fermions, where $n = 0, \pm1, \pm2, \ldots$. There is an energy conserving Kronecker delta

at each vertex: $\beta\delta_{p^0_{in},p^0_{out}}$. In any given diagram there will be one factor of $\beta(2\pi)^3\delta^3(0) \to \beta V$ left over. Literally the diagramatic expansion is for $\beta V\Omega_I$, not Ω_I.

Finally there is an integral-sum for each line: $T\sum_n \int d^3\ell/(2\pi)^3$. It turns out to be useful to express this sum as a contour integral.[13,15] For bosons,

$$T\sum_n f(k^0 = 2\pi niT) = \frac{1}{2\pi i}\int_{-i\infty+\varepsilon}^{i\infty+\varepsilon} dk^0 \frac{1}{\exp(\beta k_0)-1}\left[f(k^0)+f(-k^0)\right] + \frac{1}{2\pi i}\int_{-i\infty}^{i\infty} dk^0\, f(k^0) \quad ; \tag{2.7}$$

and for fermions,

$$T\sum_n f(p^0 = (2n+1)\pi iT+\mu) = -\frac{1}{2\pi i}\int_{-i\infty+\mu+\varepsilon}^{i\infty+\mu+\varepsilon} dp^0 \frac{1}{\exp[\beta(p^0-\mu)]+1} f(p^0) - \frac{1}{2\pi i}\int_{-i\infty+\mu-\varepsilon}^{i\infty+\mu-\varepsilon} dp^0 \frac{1}{\exp[\beta(\mu-p^0)]+1} f(p^0) + \frac{1}{2\pi i}\oint_C dp^0 f(p^0) + \frac{1}{2\pi i}\int_{-i\infty}^{i\infty} dp^0 f(p^0) \; . \tag{2.8}$$

Here $\varepsilon > 0$ is an infinitesimal. The contour C is a strip of infinite length in the complex p^0 plane and has vertices $(0,-i\infty) \to (\mu,-i\infty) \to (\mu,i\infty) \to (0,i\infty) \to (0,-i\infty)$. It is drawn in Fig. 2. Notice that the first term on the right side of Eq. (2.7) and the first two terms on the right side of Eq. (2.8) vanish in the limit $\beta = 1/T \to \infty$. Also the third term

on the right side of Eq. (2.8) vanishes in the limit $\mu \to 0$. For this reason we refer to the first term on the right side of Eq. (2.7) and the first three terms on the right side of Eq. (2.8) as matter contours, whereas the remaining term in each equation is called the vacuum contour.

3. THERMODYNAMIC POTENTIAL TO SECOND ORDER

The diagrams[14] for the thermodynamic potential to second order in the coupling are shown in Figs. 3a-5a. The brackets indicate that the enclosed subgraph is renormalized. After the pure vacuum contributions to each graph are subtracted off, these diagrams yield a finite contribution to Ω_I. The diagrams shown in Figs. 3a-5a will be evaluated in Sections 3.1 to 3.3 respectively. In Section 3.4 we examine the second order contribution to the thermodynamic potential for various limiting cases.

3.1 Fermion Loop

The diagrams in Fig. 3a can be redrawn as in Fig. 3b. The parentheses indicate that the enclosed subgraph is evaluated in the vacuum, and the lines entering and leaving the subgraph are evaluated on the mass shell while in the subgraph. Thus the subgraph in brackets plus the subgraph in parentheses equal the subgraph with no brackets or parentheses around it.

There are two methods of doing explicit calculations with these diagrams. The traditional method is to perform the energy sums directly. Another method is to perform analytic continuations and employ the contour integrals of Eqs. (2.8) and (2.9). Both methods will be used in this section to show that they give identical results, and in the process it will become clear which method is easier to use.

Consider the first diagram of Fig. 3a. It is

$$\tfrac{1}{2} g^2 \tau^a_{ij} \tau^{ij}_a \int \frac{d^3k}{(2\pi)^3} \frac{d^3p}{(2\pi)^3} \frac{d^3q}{(2\pi)^3} (2\pi)^3 \delta^3(\underset{\sim}{p} - \underset{\sim}{q} - \underset{\sim}{k})$$

$$\times \frac{1}{\beta} \sum_{n_k} \frac{1}{\beta} \sum_{n_p} \frac{1}{\beta} \sum_{n_q} \beta \delta_{n_p, n_q + n_k} \frac{\mathrm{Tr}\gamma^\mu (\not{p}+m)\gamma_\mu(\not{q}+m)}{k^2(p^2-m^2)(q^2-m^2)} \quad . \tag{3.1}$$

For simplicity we will work in the Feynman gauge, $\alpha = 1$. This choice will be discussed later. We recall that

$$\tau^a_{ij} \tau^{ij}_a = \mathrm{Tr}\, \tau^a \tau_a = \tfrac{1}{2} N_g \quad , \tag{3.2}$$

where $N_g = N_c^2 - 1$ is the number of gluons for the color gauge group $SU(N_c)$.

Let us first perform the summations directly. The relevant part of Eq. (3.1) is

$$-\frac{8}{\beta^2} \sum_{n_k} \sum_{n_p} \sum_{n_q} \frac{2m^2 + \underset{\sim}{p} \cdot \underset{\sim}{q} + \big((2n_p+1)\pi/\beta - i\mu\big)\big((2n_q+1)\pi/\beta - i\mu\big)}{[(2\pi n_k/\beta)^2 + \omega^2][\big((2n_p+1)\pi/\beta - i\mu\big)^2 + E_p^2][\big((2n_q+1)\pi/\beta - i\mu\big)^2 + E_q^2]}$$

$$\times \delta_{n_p, n_q + n_k} \quad . \tag{3.3}$$

Here $E_p \equiv \sqrt{\underset{\sim}{p}^2 + m^2}$ and $\omega \equiv \sqrt{\underset{\sim}{k}^2}$. It is most convenient to use the Kronecker delta to eliminate the n_k summation. The idea then is to use the method of partial fractions to write Eq. (3.3) as a sum of terms of the form

$$\sim \sum_{n_p} \frac{1}{n_p + a + ib} \sum_{n_q} \frac{1}{n_q + a + ic} \frac{1}{n_q - n_p + id} \quad , \tag{3.4}$$

where a, b, c and d are all real. In this problem there will be eight such terms. Equation (3.4) is evaluated with the aid of the relation[24]

$$\sum_{n=-\infty}^{\infty} \frac{1}{(n-\theta)(n-\phi)} = \frac{\pi(\cot\pi\theta - \cot\pi\phi)}{\phi - \theta} \quad . \tag{3.5}$$

All that remains is to do the straightforward but very tedious algebra. The result of performing the sum in Eq. (3.3) turns out to be

$$\frac{1}{4E_pE_q\omega}\left(2m^2 - E_pE_q + \underset{\sim}{p}\cdot\underset{\sim}{q}\right)\left\{\frac{\omega}{(E_p-E_q)^2-\omega^2}\left[\tanh\frac{\beta(E_q-\mu)}{2}\tanh\frac{\beta(E_p-\mu)}{2}\right.\right.$$

$$\left.+\tanh\frac{\beta(E_q+\mu)}{2}\tanh\frac{\beta(E_p+\mu)}{2}\right]+\frac{\omega}{(E_p+E_q)^2-\omega^2}$$

$$\times\left[\tanh\frac{\beta(E_q-\mu)}{2}\tanh\frac{\beta(E_p+\mu)}{2}+\tanh\frac{\beta(E_q+\mu)}{2}\tanh\frac{\beta(E_p-\mu)}{2}\right]$$

$$+E_q\left[\frac{1}{(E_p-\omega)^2-E_q^2}+\frac{1}{(E_p+\omega)^2-E_q^2}\right]\coth\frac{\beta\omega}{2}\left[\tanh\frac{\beta(E_p-\mu)}{2}\right.$$

$$\left.\left.+\tanh\frac{\beta(E_p+\mu)}{2}\right]-\frac{8\,E_p\,E_q\,\omega}{[(E_p+E_q)^2-\omega^2][(E_p-E_q)^2-\omega^2]}\right\}+\frac{1}{(E_p+E_q)^2-\omega^2}$$

$$\times\left[1+\tanh\frac{\beta(E_p+\mu)}{2}\tanh\frac{\beta(E_q-\mu)}{2}\right]-\frac{1}{(E_p+E_q)^2-\omega^2}\;\frac{E_p+E_q}{\omega}$$

$$\times\coth\frac{\beta\omega}{2}\left[\tanh\frac{\beta(E_q-\mu)}{2}+\tanh\frac{\beta(E_p-\mu)}{2}\right]+E_p\leftrightarrow E_q\ . \qquad (3.6)$$

An annoying feature of doing the sum explicitly is that the hyperbolic functions do not naturally occur with arguments $\beta(E_p-\mu)/2$ etc., but rather, arguments such as $\beta(E_p-\mu+\omega)/2$ also occur. Hyperbolic identities must be used to put them in natural form.

Using the relations

$$\tanh\frac{\beta(E_p\pm\mu)}{2}=1-2n_p^{\pm}\ ,\qquad n_p^{\pm}\equiv\frac{1}{\exp\beta(E_p\pm\mu)+1}\ ,\qquad n_p\equiv n_p^{+}+n_p^{-}\ ,$$

(3.7a)

$$\coth \frac{\beta\omega}{2} = 1 + 2N_k \quad , \qquad N_k \equiv \frac{1}{\exp\beta\omega - 1} \quad , \tag{3.7b}$$

the pure vacuum contribution to Eq. (3.6) may be subtracted off to give, for Eq. (3.1),

$$\tfrac{1}{4} g^2 N_g \int \frac{d^3p}{(2\pi)^3} \frac{d^3q}{(2\pi)^3} \frac{d^3k}{(2\pi)^3} (2\pi)^3 \delta^3(\underset{\sim}{p} - \underset{\sim}{q} - \underset{\sim}{k})$$

$$\times \left\{ \frac{1}{E_p E_q} \left[\frac{2m^2}{(E_p - E_q)^2 - \omega^2} + 1 \right] \left[n_q^- n_p^- + n_q^+ n_p^+ \right] \right.$$

$$+ \frac{1}{E_p E_q} \left[\frac{2m^2}{(E_p + E_q)^2 - \omega^2} + 1 \right] \left[n_q^- n_p^+ + n_q^+ n_p^- \right] + \frac{4}{E_p \omega} N_k n_p$$

$$\left. - \frac{4}{E_p \omega} N_k + \frac{2n_p}{E_p} \left[\frac{1}{\omega} - \frac{1}{E_q} + \frac{2m^2 (E_q + \omega)}{E_q \omega \left[(E_q + \omega)^2 - E_p^2 \right]} \right] \right\} \quad . \tag{3.8}$$

In obtaining this result we used the equation

$$\int d^3k \, d^3p \, d^3q \; \delta^3(\underset{\sim}{p} - \underset{\sim}{q} - \underset{\sim}{k}) \frac{N_k}{E_p E_q \omega} \left[\frac{E_p + E_q}{(E_p + E_q)^2 - \omega^2} - \frac{E_p - E_q}{(E_p - E_q)^2 - \omega^2} \right]$$

$$= \int d^3k \, d^3p \, \frac{N_k}{E_p \omega} \frac{\underset{\sim}{p} \cdot \underset{\sim}{k}}{E_p^2 \omega^2 - (\underset{\sim}{p} \cdot \underset{\sim}{k})^2} = 0 \quad , \tag{3.9}$$

on account of the fact that the integrand is odd under the transformation $\underset{\sim}{p} \to -\underset{\sim}{p}$.

Only the last two terms of Eq. (3.8) do not yield a finite answer. These infinities should be cancelled by the last two diagrams of Fig. 3b if the theory is to yield a finite answer.

The second method is to do an analytic continuation and evaluate using contour integrals. The relevant part of Eq. (3.1) is

$$8\,\frac{1}{\beta}\sum_{n_k}\frac{1}{\beta}\sum_{n_p}\frac{1}{\beta}\sum_{n_q}\beta\delta_{n_p,n_q+n_k}\;\frac{2m^2-p\cdot q}{k^2(p^2-m^2)(q^2-m^2)}\quad . \tag{3.10}$$

One's first attempt might be to eliminate one summation, say n_q, using the Kronecker delta. The remaining two summations, over n_k and n_p, would be replaced by contour integrals via Eqs. (2.9) and (2.10). When this is done, however, the result does not agree with the result, Eq. (3.8), obtained by performing the sums directly. Indeed the result depends on which sum in Eq. (3.10) is eliminated and on which order the two contour integrations are performed! This indicates that the procedure as it stands is mathematically ill-defined.

The root of the problem is the fact that there is no unique analytic continuation of a function which is defined only on the integers. In fact there exists an infinite number of analytic continuations. This ambiguity seems to have gone unnoticed by some papers in the literature.[13,15] The resolution of the ambiguity is discussed by Norton and Cornwall.[25] The arguments in that paper apply specifically to bosons but may easily be generalized to fermions. The Kronecker delta may be written as

$$\beta\delta_{n_p,n_q+n_k} = \int_0^\beta du\,\exp u(p^0-q^0-k^0) = \frac{\exp\beta(p^0-q^0-k^0)-1}{p^0-q^0-k^0}\quad , \tag{3.11}$$

when $p^0 = (2n_p+1)\pi i/\beta+\mu$, $q^0 = (2n_q+1)\pi i/\beta+\mu$, $k^0 = 2n_k\pi i/\beta$. Since q^0 and k^0 enter the argument of the exponentials in Eq. (3.11) with a negative sign we multiply by $-\exp\beta(q^0-\mu+k^0)$, which is unity when evaluated on

the integers. This prescription ensures that the integrands of the contour integrals fall off exponentially before the u integral is performed, and so is essentially a unique prescription. This prescription also ensures that the normal vacumm is recovered in the limit of zero temperature and chemical potential.

With this choice of analytic continuation, Eq. (3.10) becomes

$$8\,\frac{1}{\beta}\sum_{n_k}\frac{1}{k^2}\,\frac{1}{\beta}\sum_{n_p}\frac{1}{p^2-m^2}\,\frac{1}{\beta}\sum_{n_q}\frac{1}{p^2-m^2}\;I(p^0,q^0,k^0)\qquad ,$$

$$I(p^0,k^0,q^0)\;\equiv\;\frac{2m^2-p\cdot q}{p^0-q^0-k^0}\left[\exp\beta(q^0-\mu+k^0)-\exp\beta(p^0-\mu)\right]. \qquad (3.12)$$

Notice that I has no singularities. Hence each of the sums may be converted to a contour integral via Eqs. (2.9) and (2.10), and these integrals may be performed independently of each other with no ambiguity. For example,

$$\frac{1}{\beta}\sum_{n_p}\frac{1}{p^2-m^2}\,I(p^0,q^0,k^0)\;=\;\frac{1}{2E_p}\,I(E_p,q^0,k^0)n_p^-+\frac{1}{2E_p}\,I(-E_p,q^0,k^0)(n_p^+-1)\;, \qquad (3.13a)$$

$$\frac{1}{\beta}\sum_{n_k}\frac{1}{k^2}\,I(p^0,q^0,k^0)\;=\;-\frac{1}{2\omega}\,I(p^0,q^0,\omega)N_k-\frac{1}{2\omega}\,I(p^0,q^0,-\omega)(N_k+1)\;. \qquad (3.13b)$$

Then Eq. (3.12) can be written as

$$- \frac{1}{E_p E_q \omega} \Big\{ n_p^- n_q^- \left[N_k I(E_p, E_q, \omega) + (N_k + 1)\ I(E_p, E_q, -\omega) \right]$$

$$+ n_p^- (n_q^+ - 1) \left[N_k\ I(E_p, -E_q, \omega) + (N_k + 1)\ I(E_p, -E_q, -\omega) \right]$$

$$+ n_q^- (n_p^+ - 1) \left[N_k\ I(-E_p, E_q, \omega) + (N_k + 1)\ I(-E_p, E_q, -\omega) \right]$$

$$+ (n_p^+ - 1)(n_q^+ - 1) \left[N_k\ I(-E_p, -E_q, \omega) + (N_k + 1)\ I(-E_p, -E_q, -\omega) \right] \Big\} \ . \tag{3.14}$$

The exponentials contained in the I's may be written in terms of the n's and N by using

$$\exp \beta(E_p \pm \mu) = 1 / n_p^{\pm} - 1 \quad , \tag{3.15a}$$

$$\exp \beta\omega = 1 / N_k + 1 \quad . \tag{3.15b}$$

The algebra to simplify Eq. (3.14) is much less lengthy than that encountered when simplifying the corresponding expression in the direct summation method. After subtracting off a pure vacuum contribution Eq. (3.14) reduces to Eq. (3.8) so that, in fact, the two methods give identical answers.

The contour integral method has two advantages over the direct summation method. These advantages become more pronounced as the complexity of the diagram increases. The contour integrals may be evaluated independently of each other. In fact Eq. (3.13) is quite general, and should hold for more complicated diagrams as well. Conversely, the direct summations must be done in consecutive order. Also the contour integral method directly expresses the diagram in terms

of the n's and N's, whereas the direct summation method yields intermediate results involving hyperbolic functions with arguments which mix different energies (i.e. $E_p - \mu + \omega$ instead of $E_p - \mu$ and ω).

To finish the fermion loop calculation we must evaluate the last two diagrams of Fig. 3b. Consider the first of them. The subgraph is

$$\lim_{\substack{\beta\to\infty \\ \mu\to 0}} g^2 \tau^a_{ij} \tau^{ij}_a \int \frac{d^3p}{(2\pi)^3} \frac{d^3q}{(2\pi)^3} (2\pi)^3 \delta^3(\underset{\sim}{p} - \underset{\sim}{q} - \underset{\sim}{k}) \frac{1}{\beta} \sum_{n_p} \frac{1}{\beta} \sum_{n_q} \frac{1}{p^2-m^2} \frac{1}{q^2-m^2}$$

$$\times \quad \mathrm{Tr} \frac{\gamma^\mu(\not{p}+m)\gamma^\nu(\not{q}+m)}{p^0 - q^0 - k^0} \left[\exp\beta(q^0 - \mu + k^0) - \exp\beta(p^0 - \mu)\right] \tag{3.16}$$

because the parentheses mean that we should take the zero temperature and chemical potential limit. In addition we should evaluate the gluon on the mass shell, $k^2=0$. It is actually more convenient not to do so at this point. The reason is that the contour integral method puts each particle on its mass shell automatically. If the subgraph was evaluated using the usual vacuum Feynman rules the relevant particles would have to be put on shell by hand.

Since we are working in the Feynman gauge we may as well multiply by $g_{\mu\nu}$ to simplify the algebra. The relevant part of Eq. (3.16) becomes

$$\lim_{\substack{\beta\to\infty \\ \mu\to 0}} \frac{1}{\beta} \sum_{n_p} \frac{1}{p^2-m^2} \frac{1}{\beta} \sum_{n_q} \frac{1}{q^2-m^2} \frac{8(2m^2 - p\cdot q)}{p^0 - q^0 - k^0} \left[\exp\beta(q^0 - \mu + k^0) - \exp\beta(p^0 - \mu)\right] . \tag{3.17}$$

This is readily evaluated with the aid of Eqs. (3.13a) and (3.15a). The result is

$$\frac{2(2m^2 + E_p E_q + \underset{\sim}{p}\cdot\underset{\sim}{q})}{E_p E_q} \left\{ \frac{1}{E_p + E_q - k_0} + \frac{\exp \beta k_0}{E_p + E_q + k^0} \right\} . \tag{3.18}$$

The factor $\exp\beta k_0$ is left alone since it does not properly belong to the subgraph only. When this expression for the subgraph is inserted back into the second diagram, and use is made of Eqs. (3.13b), (3.15b), and (3.9), we obtain

$$g^2 N_g \int \frac{d^3p}{(2\pi)^3} \frac{d^3k}{(2\pi)^3} \frac{N_k}{E_p \omega} \quad . \tag{3.19}$$

This is readily seen to exactly cancel the second to last term of Eq. (3.8), which was infinite.

Finally, consider the last diagram of Fig. 3b. The subgraph is

$$\lim_{\substack{\beta\to\infty \\ \mu\to 0}} \tfrac{1}{2} g^2 N_g \int \frac{d^3q}{(2\pi)^3} \frac{d^3k}{(2\pi)^3} (2\pi)^3 \delta^3(\underset{\sim}{p} - \underset{\sim}{q} - \underset{\sim}{k}) \frac{1}{\beta} \sum_{n_q} \frac{1}{q^2 - m^2}$$

$$\times \frac{1}{\beta} \sum_{n_k} \frac{1}{k^2} \frac{\gamma^\mu (\not{q} + m)\gamma_\mu}{p^0 - q^0 - k^0} \left[\exp\beta(q^0 - \mu + k^0) - \exp\beta(p^0 - \mu)\right] \quad . \tag{3.20}$$

Following the analogous steps that led to Eq. (3.18), we get

$$-\tfrac{1}{4} g^2 N_g \int \frac{d^3q}{(2\pi)^3} \frac{d^3k}{(2\pi)^3} (2\pi)^3 \delta^3(\underset{\sim}{p} - \underset{\sim}{q} - \underset{\sim}{k}) \frac{1}{E_q \omega}$$

$$\times \left\{ \frac{2m - \not{q}}{p^0 - E_q - \omega} \bigg|_{q^0 = E_q} + \exp\beta(p^0 - \mu) \frac{2m - \not{q}}{p^0 + E_q + \omega} \bigg|_{q^0 = -E_q} \right\} \quad . \tag{3.21}$$

When this expression for the subgraph is inserted back into the diagram, and Eq. (3.13a) is used to evaluate the final fermion line, we find

$$\tfrac{1}{2} g^2 N_g \int \frac{d^3p}{(2\pi)^3} \frac{d^3q}{(2\pi)^3} \frac{d^3k}{(2\pi)^3} (2\pi)^3 \delta^3(\underset{\sim}{p} - \underset{\sim}{q} - \underset{\sim}{k}) \frac{n_p}{E_p}$$

$$\times \left[-\frac{1}{\omega} + \frac{1}{E_q} - \frac{2m^2 (E_q + \omega)}{E_q \omega \left[(E_q + \omega)^2 - E_p^2\right]} \right] \quad . \tag{3.22}$$

This cancels the last term, and final infinity, of Eq. (3.8).

The purpose of going into so much detail in this evaluation is twofold. First is to show the power and simplicity of the contour integral method. No explicit sums or energy integrals need to be done, since Eq. (3.13) is done once and for all and can be applied to each line in a given diagram. It should be noted, though, that if one works in a gauge other than Feynman there will be double poles due to the gluon propagator $[g^{\mu\nu} - (1-\alpha)k^\mu k^\nu/k^2]/k^2$. Equations (3.13b) must then be replaced by a more complicated expression. The second point is to notice how the ultraviolet divergencies cancelled. The bare diagram of Fig. 3b had the from

$$\int d^3p\, d^3k[(\ )Nn + (\ )nn + (\ )N + (\ )n + (\ )] \quad .$$

The last term was a purely vacuum term and was thrown away. The N and n terms were exactly cancelled by the two counterterm diagrams of Fig. 3b. We expect this structure and cancellation of ultraviolet divergences to repeat in higher order diagrams. Infrared divergences, when and if they appear, will have an entirely different structure.

The final expression for the fermion loop diagrams is

$$\Omega^{\text{exch}}_{(2)} = \frac{4}{3}\pi\alpha_c N_g T^2 \sum_f \int \frac{d^3p}{(2\pi)^3}\frac{n_p}{E_p} + 4\pi\alpha_c N_g \sum_f \int \frac{d^3p}{(2\pi)^3}\frac{d^3q}{(2\pi)^3}$$

$$\times \frac{1}{E_p E_q}\left\{\left[\frac{2m^2}{(E_p - E_q)^2 - \omega^2} + 1\right]\left[n_q^- n_p^- + n_q^+ n_p^+\right]\right.$$

$$\left. + \left[\frac{2m^2}{(E_p + E_q)^2 - \omega^2} + 1\right]\left[n_q^- n_p^+ + n_q^+ n_p^-\right]\right\} \quad , \qquad (3.23)$$

where the color gauge structure constant is defined as $\alpha_c \equiv g^2/16\pi$, and $\omega = |\underset{\sim}{p} - \underset{\sim}{q}|$ in the second integral. In this equation there is a sum over all quark flavors. In general the masses m_f and chemical potentials μ_f need not be identical. Except for a factor $N_g/2$ this is the same expression that arises in quantum electrodynamics.[18] It is referred to as the exchange contribution because it arises, in the zero temperature limit, from a pair of fermions exchanging their three-momenta in the Fermi sea.

3.2 Ghost Loop

The diagrams in Fig. 4a can be redrawn as in Fig. 4b. We shall evaluate these using the contour integral method only.

The first diagram of Fig. 4b is

$$\tfrac{1}{2} g^2 f_{abc} f^{abc} \int \frac{d^3p}{(2\pi)^3} \frac{d^3q}{(2\pi)^3} \frac{d^3k}{(2\pi)^3} (2\pi)^3 \delta^3(\underset{\sim}{p} - \underset{\sim}{q} - \underset{\sim}{k})$$

$$\times \frac{1}{\beta} \sum_{n_p} \frac{1}{\beta} \sum_{n_q} \frac{1}{\beta} \sum_{n_k} \frac{p \cdot q}{p^2 q^2 k^2} \frac{\exp \beta p^0 - \exp \beta(q^0 + k^0)}{p^0 - q^0 - k^0} . \tag{3.24}$$

Defining

$$J(p^0, q^0, k^0) \equiv \frac{p \cdot q}{p^0 - q^0 - k^0} \left[\exp\beta p^0 - \exp\beta(q^0 + k^0)\right] , \tag{3.25}$$

and using Eq. (3.13b), the relevant part of Eq. (3.24) becomes

$$- \frac{1}{16\,\omega_p\omega_q\omega_k} \Big\{ N_p N_q \left[N_k\ J(\omega_p,\omega_q,\omega_k) + (N_k+1)\ J(\omega_p,\omega_q,-\omega_k)\right]$$

$$+\ N_p(N_q+1)\ \left[N_k\ J(\omega_p,-\omega_q,\omega_k) + (N_k+1)\ J(\omega_p,-\omega_q,-\omega_k)\right]$$

$$+\ (N_p+1)N_q\ \left[N_k\ J(-\omega_p,\omega_q,\omega_k) + (N_k+1)\ J(-\omega_p,\omega_q,-\omega_k)\right]$$

$$+\ (N_p+1)(N_q+1)\ \left[N_k\ J(-\omega_p,-\omega_q,\omega_k) + (N_k+1)\ J(-\omega_p,-\omega_q,-\omega_k)\right]\Big\}\ . \tag{3.26}$$

Making use of Eq. (3.15b) and making some trivial transformations this becomes

$$\tfrac{1}{4}\,\frac{N_q}{\omega_q}\,\frac{N_p}{\omega_p} + \tfrac{1}{4}\,\frac{1}{\omega_q}\,\frac{N_p}{\omega_p}\ . \tag{3.27}$$

The second and third graphs of Fig. 4b contribute $-N_p/4\omega_p\omega_q$ and 0 respectively. Hence the whole of Fig. 4b is evaluated as

$$\tfrac{1}{4}\,g^2\,f_{abc}\,f^{abc}\int \frac{d^3p}{(2\pi)^3}\,\frac{d^3q}{(2\pi)^3}\,\frac{N_p N_q}{\omega_p\,\omega_q} = \frac{g^2\,N_c\,N_g}{576}\,T^4\ . \tag{3.28}$$

The product of structure constants $f_{abc}\,f^{abc}$ is $N_c N_g$ for color $SU(N_c)$. Notice that, as in the fermion loop calculation, all the ultraviolet divergences have cancelled.

3.3 Gluon Loop

The diagrams in Fig. 5a can be redrawn as in Fig. 5b. Again we shall evaluate these using the contour integral method. The steps to evaluate the diagrams should be familiar by now. Hence we only quote the results. Apart from a factor of $g^2N_cN_g$ and the integration over

three-momenta, the four diagrams of Fig. 5b are, respectively,

$$-\frac{1}{12}\left\{\frac{27}{\omega_p\omega_q}\,N_p(N_q+1)\right\}\quad, \tag{3.29a}$$

$$\frac{1}{4}\left\{\frac{9}{\omega_p\omega_q}\,N_p\right\}\quad, \tag{3.29b}$$

$$-\frac{1}{8}\left\{\frac{-24}{\omega_p\omega_q}\,N_p(N_q+1)\right\}\quad, \tag{3.29c}$$

$$\frac{1}{4}\left\{\frac{-12}{\omega_p\omega_q}\,N_p\right\}\quad. \tag{3.29d}$$

The ultraviolet divergences cancel leaving the finite result

$$\frac{3}{4}g^2 N_c N_g \int \frac{d^3p}{(2\pi)^3}\,\frac{d^3q}{(2\pi)^3}\,\frac{N_p N_q}{\omega_p\omega_q} = \frac{g^2 N_c N_g}{192}\,T^4\quad. \tag{3.30}$$

3.4 Limiting Cases

The full second order contribution to the thermodynamic potential is given by

$$\Omega_{(2)} = \Omega_{(2)}^{\text{exch}} + \Omega_{(2)}^{\text{glue}}\quad, \tag{3.31}$$

where $\Omega_{(2)}^{\text{exch}}$ is given by Eq. (3.23), and $\Omega_{(2)}^{\text{glue}}$ is given by the sum of Eqs. (3.28) and (3.30):

$$\Omega_{(2)}^{\text{glue}} = \frac{\alpha_c\pi}{9}\,N_c N_g\,T^4\quad. \tag{3.32}$$

We refer to this as a "glue" contribution since it involves no fermions.

Its contribution to the pressure of the system is negative ($P = -\Omega$) as befits the name gluon for the gauge vector meson. For completeness we quote the expression for the thermodynamic potential in the absence of interactions:

$$\Omega_{(0)} = -\frac{2}{3} N_c \sum_f \int \frac{d^3p}{(2\pi)^3} \frac{\underset{\sim}{p}^2}{E_p} n_p - \frac{\pi^2}{45} N_g T^4 \quad . \tag{3.33}$$

Since the pieces involving fermions cannot be expressed in terms of elementary functions, it is useful to consider various limiting cases. Consider for the moment only one flavor of quark.

In the ultrarelativistic ($m = 0$) and zero temperature limit,

$$\Omega = \frac{-\mu^4}{12\pi^2} N_c \left[1 - \frac{3\alpha_c}{\pi} \frac{N_g}{N_c} \right] \quad . \tag{3.34}$$

In the ultrarelativistic ($m = 0$) and zero chemical potential limit,

$$\Omega = -\frac{\pi^2 T^4}{45} \left(N_g + \frac{7}{4} N_c \right) \left[1 - \frac{45}{9} \frac{\alpha_c}{\pi} \frac{N_g (N_c + 5/4)}{(N_g + 7/4\ N_c)} \right] \quad . \tag{3.35}$$

In the nonrelativistic, classical statistics limit,

$$\Omega = -\frac{2N_c}{(2\pi)^{3/2}} (m^3 T^5)^{1/2} \exp(-\mu'/T) \left[1 + \alpha_c \frac{N_g}{N_c} \left(\frac{2m}{\pi T} \right)^{1/2} \exp(-\mu'/T) \right] , \tag{3.36}$$

$$\mu' \equiv m - \mu \quad .$$

Finally a word needs to be said about our choice of gauge. We worked in the Feynman gauge, $\alpha = 1$, for computational simplicity. The relationship between the Feynman gauge and an arbitrary covariant gauge α is $g^2(1) = g^2(\alpha) + \mathcal{O}\left(g^4(\alpha)\right)$. Furthermore, since the perturbation

expansion for the thermodynamic potential is gauge-invariant (see Section 2), it is easily seen that the second order contribution must be gauge-invariant. However at any given order equal to or greater than four the contribution will be gauge-dependent.

4. THERMODYNAMIC POTENTIAL TO THIRD ORDER

There is a contribution to the thermodynamic potential which is of higher order in the coupling than g^2 but less than g^4. This is a nonperturbative effect which arises from interactions giving the gluons a mass. (In this regard, see also Ref. 26). This has customarily been called the plasmon effect in many-body physics.

The diagrams which contribute to this order are shown in Fig. 6. This is a formal expansion. The series must be summed nonperturbatively because of the divergence at $k^2 = 0$.

$$\Omega^{cor} = \frac{1}{2}\,\frac{1}{\beta}\sum_{n_k}\int \frac{d^3k}{(2\pi)^3}\ \mathrm{Tr}\Big[\log\big(1 + D_o(k)\pi_R^{(2)}(k)\big) - D_o\pi_R^{(2)}(k)\Big]. \tag{4.1}$$

This gluon correlation expression contributes to both the plasmon term and to terms of fourth order. $\pi_R^{(2)}(k)$ represents the renormalized gluon polarization tensor to second order at arbitrary temperature and chemical potential. In the remainder of this section we drop the subscript R and the superscript (2) for notational convenience. $\pi(k)$ may be decomposed as

$$\pi(k) = \pi_{vac}(k) + \pi_{mat}(k) \quad , \tag{4.2}$$

where

$$\pi_{vac}(k) = \lim_{\beta\to\infty}\ \lim_{\mu\to\infty}\ \pi(k) \quad , \tag{4.3}$$

and $\pi_{mat}(k)$ is the piece which exists only at finite temperature and/or chemical potential.

To separate out the plasmon contribution to Ω^{cor} it is convenient to write it as

$$\Omega^{cor} = \frac{1}{2}\frac{1}{\beta}\sum_{n_k}\int \frac{d^3k}{(2\pi)^3}\left[\mathrm{Tr}\,\log\left(1 + \frac{1}{1+D_o(k)\,\pi_{vac}(k)}\;D_o(k)\,\pi_{mat}(k)\right)\right.$$

$$\left. + \;\mathrm{Tr}\,\log\left(1 + D_o\pi_{vac}(k)\right) - D_o\pi(k)\right] \quad . \tag{4.4}$$

At zero temperature the second term is a pure vacuum contribution and should be subtracted off, but not at finite temperature. Expanding the denominator in the first term and the logarithm in the second, we get, to this order,

$$\Omega^{cor} = \frac{1}{2}\frac{1}{\beta}\sum_{n_k}\int \frac{d^3k}{(2\pi)^3}\left[\mathrm{Tr}\,\log\left(1 + D_o(k)\,\pi_{mat}(k)\right) - D_o(k)\,\pi_{mat}(k)\right.$$

$$\left. - \;\frac{1}{2}\,D_o(k)\,\pi_{vac}(k)\;\;D_o(k)\,\pi_{vac}(k) - D_o(k)\,\pi_{vac}(k)\;\;D_o(k)\,\pi_{mat}(k)\right] \; . \tag{4.5}$$

The last two terms are infrared convergent, are of order g^4, and will be discussed further in the next section.

The trace over the logarithm in Eq. (4.5) needs to be done. From rotational invariance and current conservation $\pi_{mat}(k)$ has the form

$$\pi^{\mu\nu,ab}_{mat}(k) = (k^\mu k^\nu - g^{\mu\nu}k^2)\,\frac{1}{\underset{\sim}{k}^2}\;\pi^{0,ab}_{mat\;0}(k) + g^{\mu i}\left(k_i k_j - \delta_{ij}\,\underset{\sim}{k}^2\right)g^{j\nu}$$

$$\times\;\frac{1}{2\underset{\sim}{k}^2}\left(\pi^{\mu,ab}_{mat\,\mu}(k) + \frac{3k^2}{\underset{\sim}{k}^2}\;\pi^{0,ab}_{mat\;0}(k)\right) \tag{4.6}$$

Furthermore, the overall color index dependence must be δ^{ab}. $\pi_{mat}(k)$ can then be written as a linear combination of the transverse and longitudinal projection tensors defined by[26]

$$P^T_{00} = P^T_{0i} = P^T_{i0} = 0 \quad ,$$

$$P^T_{ij} = \delta_{ij} - \frac{k_i k_j}{\underset{\sim}{k}^2} \quad ,$$

$$P^L_{\mu\nu} = \frac{k_\mu k_\nu}{k^2} - g_{\mu\nu} - P^T_{\mu\nu} \quad . \tag{4.7}$$

They have the following important properties:

$$P^T_{\mu\nu} P^{\mu\nu}_L = 0 \quad ,$$

$$P^L_{\mu\sigma} P^{\sigma\nu}_L = -P^{L\nu}_\mu \quad ,$$

$$P^T_{\mu\sigma} P^{\sigma\nu}_T = -P^{T\nu}_\mu \quad ,$$

$$P^\mu_{T\,\mu} = -2 \quad ,$$

$$P^\mu_{L\,\mu} = -1 \quad . \tag{4.8}$$

After performing the trace the first two terms of Eq. (4.5) become

$$\frac{1}{2} N_g \frac{1}{\beta} \sum_n \int \frac{d^3k}{(2\pi)^3} \left[\log\left(1 + \frac{g^2}{\omega^2} \Lambda_1(n,\omega)\right) - \frac{g^2}{\omega^2} \Lambda_1(n,\omega) \right.$$

$$\left. + 2\log\left(1 + \frac{g^2}{\omega^2} \Lambda_2(n,\omega)\right) - \frac{2g^2}{\omega^2} \Lambda_2(n,\omega) \right] \quad , \tag{4.9}$$

where

$$g^2 \Lambda_1(n,\omega) = -\frac{1}{N_g} \pi^{0,aa}_{mat\,0}(k) \quad ,$$

$$g^2 \Lambda_2(n,\omega) = \frac{1}{2N_g} \left(\pi^{0,aa}_{mat\,0}(k) + \frac{\omega^2}{k^2} \pi^{\mu,aa}_{mat\,\mu}(k) \right) \quad ,$$

$$\omega = |\underset{\sim}{k}| \quad ,$$

$$n = n_k \quad . \tag{4.10}$$

An explicit calculation in the Feynman gauge reveals that

$$\pi^{0,aa}_{mat\,0}(k) = -\frac{N_g}{2}\frac{g^2}{\pi^2}\,\mathrm{Re}\int_0^\infty \frac{dpp^2}{E_p}\,n_p\left[1 + \frac{\omega^2 + (2\pi nT)^2 - 4E_p^2 + 4E_p(2\pi nT)i}{4p\omega}\right.$$

$$\times\ \log\left(\frac{\omega^2 + (2\pi nT)^2 - 2p\omega + 4\pi nTE_p i}{\omega^2 + (2\pi nT)^2 + 2p\omega + 4\pi nTE_p i}\right)\Bigg] - \frac{N_c N_g}{4}\frac{g^2}{\pi^2}\frac{1}{\omega}$$

$$\times\ \mathrm{Re}\int_0^\infty dq\,N_q\left[4q\omega + \left(2\omega^2 + 8\pi nTqi - 4q^2 + (2\pi nT)^2\right)\right.$$

$$\times\ \log\left(\frac{\omega^2 + (2\pi nT)^2 - 2\omega q + 4\pi nTqi}{\omega^2 + (2\pi nT)^2 + 2\omega q + 4\pi nTqi}\right)\Bigg] \quad , \tag{4.11}$$

and that

$$\pi^{\mu,aa}_{mat\,\mu}(k) = -\frac{N_g}{2}\frac{g^2}{\pi^2}\,\mathrm{Re}\int_0^\infty \frac{dpp^2}{E_p}\,n_p\left[2 + \frac{\omega^2 + (2\pi nT)^2 - 2m^2}{2p\omega}\right.$$

$$\times\ \log\left(\frac{\omega^2 + (2\pi nT)^2 - 2p\omega + 4\pi nTE_p i}{\omega^2 + (2\pi nT)^2 + 2p\omega + 4\pi nTE_p i}\right)\Bigg] - \frac{N_c N_g}{4}\frac{g^2}{\pi^2}\frac{1}{\omega}$$

$$\times\ \mathrm{Re}\int_0^\infty dq\,N_q\left[8q\omega + 5\left(\omega^2 + (2\pi nT)^2\right)\right.$$

$$\times\ \log\left(\frac{\omega^2 + (2\pi nT)^2 - 2\omega q + 4\pi nTqi}{\omega^2 + (2\pi nT)^2 + 2\omega q + 4\pi nTqi}\right)\Bigg] \quad . \tag{4.12}$$

The real parts have been taken since the imaginary parts cannot contribute to fourth order or less.

The order $|g|^3$ contribution to Eq. (4.9) is

$$\Omega^{plas}_{(3)} = \frac{1}{2} N_g \frac{1}{\beta} \sum_n \int \frac{d^3k}{(2\pi)^3} \left[\log\left(1 + \frac{g^2}{\omega^2} \Lambda_1(n,0)\right) - \frac{g^2}{\omega^2} \Lambda_1(n,0)\right.$$

$$\left. + \; 2\log\left(1 + \frac{g^2}{\omega^2} \Lambda_2(n,0)\right) - \frac{2g^2}{\omega^2} \Lambda_2(n,0)\right] , \tag{4.13}$$

and the g^4 contribution is

$$\frac{1}{2} N_g \, g^4 \frac{1}{\beta} \sum_n \int \frac{d^3k}{(2\pi)^3} \frac{1}{\omega^4} \left[\frac{1}{2} \Lambda_1^2(n,0) - \frac{1}{2} \Lambda_1^2(n,\omega) + \Lambda_2^2(n,0) - \Lambda_2^2(n,\omega)\right]. \tag{4.14}$$

In this last expression we expanded the logarithms to second order since no infrared divergence occurs.

The integral over $\underset{\sim}{k}$ in Eq. (4.13) may now be done with the result that

$$\Omega^{plas}_{(3)} = - \frac{|g|^3}{12\pi} N_g \, T \sum_n \left[\Lambda_1^{3/2}(n,0) + \Lambda_2^{3/2}(n,0)\right] . \tag{4.15}$$

In fact it is easy to check that the $\Lambda_1^{3/2}(0,0)$ term is the only nonvanishing term in the series. Hence

$$\Omega^{plas}_{(3)} = - \frac{8}{3\pi^2\sqrt{2\pi}} \alpha_c^{3/2} N_g \, T \left[\frac{2}{3}\pi^2 N_c \, T^2 + \sum_f \int_0^\infty \frac{dp}{E_p} (p^2 + E_p^2) n_p\right]^{3/2} . \tag{4.16}$$

The sum on f runs over all flavors of quark. The analogous expression for QED was first derived by Akhiezer and Peletminski.[18] Although we worked explicitly in the Feynman gauge it is apparent that this expression

should be gauge-invariant, according to the discussion of Section 3. It is clear that this is a nonperturbative contribution since a function like $\alpha_c^{3/2}$ is not analytic at $\alpha_c = 0$.

In the zero mass and zero chemical potential limit, Eq. (4.16) becomes

$$\Omega_{(3)}^{plas} = -\frac{8}{9}\sqrt{\frac{\pi}{6}}\,\alpha_c^{3/2}\,(2N_c + N_f)^{3/2}\,N_g\,T^4 \quad . \tag{4.17}$$

Here N_f is the number of quark flavors. When $T = 0$ it is known[14,16,18] that the plasmon effect contributes a term proportional to $\alpha_c^2 \log \alpha_c$ rather than $\alpha_c^{3/2}$.

5. OUTLINE OF THE FOURTH ORDER

In fourth order there are many contributions to the thermodynamic potential. Most of these contributions vanish in the zero temperature limit. We will not calculate these contributions explicitly here. Rather we should like to point out what is involved in calculating to higher orders.

In Section 4 we came across several terms which contribute to fourth order. From Eq. (4.5) there is

$$-\frac{1}{2}\,\frac{1}{\beta}\sum_n \int \frac{d^3k}{(2\pi)^3}\, D_o(k)\,\pi^{(2)}_{vac}(k)\; D_o(k)\left[\pi^{(2)}(k) - \frac{1}{2}\,\pi^{(2)}_{vac}(k)\right], \tag{5.1}$$

and from Eq. (4.14) there is

$$-\frac{1}{2}\,N_g\, g^4\,\frac{1}{\beta}\sum_n \int \frac{d^3k}{(2\pi)^3}\,\frac{1}{\omega^4}\left[\frac{1}{2}\,\Lambda_1^2(n,\omega) - \frac{1}{2}\,\Lambda_1^2(n,0) + \Lambda_2^2(n,\omega) - \Lambda_2^2(n,0)\right]. \tag{5.2}$$

The fourth order contributions not contained in Fig. 6 are shown in Fig. 7. For simplicity we show only the bare diagrams and not the numerous additional "counterterm" diagrams which appear in order to cancel the ultraviolet infinities. The way this cancellation will occur should be clear from our second order calculations of Section 3. Bare diagrams will give integrals like

$$\int d^3p\; d^3q\; d^3k\;\left[(\;)\,\mathcal{n}_p\mathcal{n}_q\mathcal{n}_k + (\;)\,\mathcal{n}_p\mathcal{n}_q + (\;)\,\mathcal{n}_p + (\;)\right],$$

where $\mathcal{n}$ stands for N, n^+ or n^-. The last term is a pure vacuum contribution and should be subtracted off. The divergent second and third terms should be cancelled by the "counterterm" diagrams leaving the convergent

first term. Unfortunately such fourth order contributions will involve nontrivial numerical calculations of six-dimensional integrals if the quark masses are nonzero. Even writing down all of the equations leading up to an integral suitable for numerical calculation will be tedious. Using the contour integral method, we see that in the Feynman gauge there are two terms per line. In fourth order there generally will be six lines leading to $2^6 = 64$ terms, as opposed to $2^3 = 8$ for the second order.

Finally, the question of gauge must be faced. As discussed in Section 3 we know that the second and third order terms are functionally independent of α whereas the fourth and higher order terms are not. We worked in the $\alpha = 1$ gauge since that was most convenient. Any other gauge complicates the calculations greatly because of double poles. However, if we want to apply the renormalization group (Section 6), then a consistent calculation requires that α remain arbitrary or that $\alpha = 0$. Schematically

$$\Omega_I = \alpha_c(0)A + \alpha_c^{3/2}(0)B + \alpha_c^2(0)C(0) + \ldots.$$

$$= \alpha_c(1)A + \alpha_c^{3/2}(1)B + \alpha_c^2(1)C(1) + \ldots.$$

We computed A and B in the $\alpha = 1$ gauge but they are the same in any gauge. In contrast, $C(0) \neq C(1)$. Freedman and McLerran[14] and Baluni[16] work with $\alpha = 0$. An alternative, which does some injustice to the theory in higher order but is consistent to fourth order, is to calculate the coefficient a in

$$\alpha_c(1) = \alpha_c(0) + a\alpha_c^2(0) + \ldots.$$

and then note that $C(0) = aA + C(1)$. Possibly a and $C(1)$ are easier to compute than $C(0)$.

6. RENORMALIZATION GROUP

The renormalization group expresses the invariance of Green's functions in a quantum field theory under different renormalization prescriptions. [For a relevant review see Ref. 1.] In general the coupling constants and masses appearing in the Lagrangian become functions of the (in this case Euclidean) subtraction point M. This is a purely quantum phenomena arising from the need to renormalize the bare quantities. Renormalizability of the theory then implies, among other things, that a change in M induces a change in all the renormalized quantities so as to leave all Green's functions unchanged. If Γ_n represents a Green's function, then

$$M \frac{d}{dM} \Gamma_n = 0 \quad . \tag{6.1}$$

It is convenient[27,28] to define a quark mass $m(M)$ depending on M by

$$S^{-1}(p)_{p^2=-M^2} = m - \not{p} \quad , \tag{6.2}$$

which agrees with the free-field theory definition. In writing down the explicit form of Eq. (6.1) m/M is treated as a generalized coupling constant. The renormalization group equation is then[13,27]

$$\left[M \frac{\partial}{\partial M} + \beta_g(g, m/M, \alpha) \frac{\partial}{\partial g} + \beta_\alpha(g, m/M, \alpha) \frac{\partial}{\partial \alpha} + \gamma_m(g, m/M, \alpha)\, m \frac{\partial}{\partial m} + \gamma_n(g, m/M, \alpha)\right] \Gamma_n = 0 \quad . \tag{6.3}$$

Here g is the coupling constant, α is the gauge fixing parameter, and γ_n is the anomalous dimension of Γ_n. For more than one flavor of quark the appropriate summation over m is to be understood.

The most convenient gauge to work in from the renormalization group point of view is the Landau gauge, $\alpha = 0$. The reason is that $\beta_\alpha(g, m/M, \alpha=0) = 0$, so that $\alpha = 0$ identically for all M. Any other gauge results in an $\alpha(M)$ which varies with M. Following the discussions of the previous sections we shall work with the Landau gauge.

Equation (6.3) states explicitly that g and m_f (f stands for flavor) are functions of M. They are found by solving

$$M \frac{dg}{dM} = \beta_g(g, m_f/M) \quad , \tag{6.4a}$$

$$\frac{M}{m_f} \frac{dm_f}{dM} = \gamma_{m_f}(g, m_f/M) \quad , \tag{6.4b}$$

with no summation over f implied. The functions β_g and γ_m have been computed to lowest order in g for an SU(3) gauge theory.[27] The results are

$$\beta_g \approx \frac{-g^3}{16\pi^2}\left[11 - \frac{2}{3}\sum_f \frac{1}{1 + 5m_f^2/M^2}\right] \quad , \tag{6.5a}$$

$$\gamma_{m_f} \approx \frac{-g^2}{2\pi^2} \frac{1}{1 + 2m_f^2/M^2} \quad . \tag{6.5b}$$

These are approximate forms for the more complicated exact expressions. They have the correct limits $m_f/M \to 0$ and $m_f/M \to \infty$, and interpolate to an accuracy of several percent in between. It is easy to verify using these forms that the solution to Eq. (6.4a), correct to lowest order in g, is

$$\frac{g^2(M)}{16\pi} \equiv \alpha_c(M) = \left[\alpha_c^{-1}(M_0) + \frac{11}{\pi}\log\frac{M^2}{M_0^2} - \frac{2}{3\pi}\sum_f \log\left(\frac{M^2+5m_f^2(M)}{M_0^2+5m_f^2(M)}\right)\right]^{-1} . \tag{6.6}$$

When all quark masses are small compared to M and M_0, this reduces to the more familiar form

$$\alpha_c(M) = \left[\alpha_c^{-1}(M_0) + \frac{1}{\pi}\left(11 - \frac{2}{3}n_f\right)\log\frac{M^2}{M_0^2}\right]^{-1} , \tag{6.7}$$

with n_f the number of quark flavors. The functional form of $m_f(M)$ is found by inserting Eqs. (6.5b) and (6.6) into Eq. (6.4b). The resulting nonlinear first order differential equations must be solved numerically.

In order to solve these differential equations some initial conditions need to be specified. We need $\alpha_c(M_0)$ and $m_f(M_0)$ at some arbitrary M_0 subject to $\alpha_c(M_0) << 1$ so that perturbation theory may be trusted. These are numbers which must be obtained from experiment.

Consider Eq. (6.7) with n_f quark flavors. With an obvious definition of Λ it may be written as

$$\alpha_c(M) = \frac{\pi}{\left(11 - \frac{2}{3}n_f\right)\log\frac{M^2}{\Lambda^2}} . \tag{6.8}$$

The number Λ is frequently referred to as the scale-breaking parameter since it leads to scaling violations from the results expected from a naive parton model analysis of deep inelastic lepton-hadron scattering. It also has importance in analyzing high energy e^+e^- annihilation experiments. In analyzing the lepton-hadron scattering experiments the appropriate subtraction point is $M^2 = Q^2$, where Q^2 is the negative of the

square of the four momentum transferred to the struck quark. The most recent and detailed analysis[29] of the SLAC data indicates that $\Lambda = 500 \pm 50$ MeV, although the best choice of Λ depends strongly on the choice of scaling variable. Essentially SLAC, at the present time, does not have a broad enough range of Q^2 to pin down the best choice of scaling variable. Restricting ourselves for the moment to the special case of three flavors whose corresponding quark masses are all small compared to 5 GeV at a subtraction point of 5 GeV then leads to a value of $\alpha_c(5\text{ GeV}) = 0.0758$.

Two more bits of information may be inferred from the approximate symmetries of the hadronic Hamiltonian, PCAC and current algebra. Using these tools it has been argued that the ratios of the bare quark masses are equal to the ratios of the masses square of appropriate pseudoscalar mesons. [See Ref. 30 and references cited therein.] It turns out that

$$m_u : m_d : m_s = 1 : 1.8 : 36 \quad , \tag{6.9}$$

which is true when M is large. Here the notation is standard: u, d and s refer to the up, down and strange quark.

One final bit of information is required to specify all the initial conditions. This may be taken as the strange quark mass at a subtraction point of ~1 GeV. Most estimates yield the same value to better than a factor of two, so this bit of information has the most uncertainty in it. However, most results depend less sensitively on the precise quark masses than they do on Λ.

If one naively believed in the valence quark structure of hadrons, then

$$m_{\Omega^-} - m_{\Xi^*} \approx m_{\Xi^*} - m_{\Sigma^*} \approx 150 \text{ MeV}$$

would indicate that $m_s - m_{u,d} \approx 150$ MeV at $M \approx 1.5$ GeV. If anything like the ratios indicated in Eq. (6.9) held as low as 1.5 GeV, then one would conclude that $m_s(1.5\text{ GeV}) \gtrsim 150$ MeV. A similar analysis of the mass difference $m_{\pi^\pm} - m_{\pi^0}$, taking into approximate account the Coulomb self-energy, results in $m_d - m_u \approx 4.9$ MeV and $m_s \approx 220$ MeV at $M \approx 1$ GeV. Politzer[28] estimates that $m_s(1\text{ GeV}) \approx 375$ MeV on the basis of strange particle production in e^+e^- annihilation and the mass of the ϕ meson. (Care must be taken to distinguish the spontaneously generated quark mass contribution.) Finally the MIT bag model fits[11] the low lying hadron spectrum with $m_u = m_d = 0$ and $m_s = 279$ MeV. On the basis of all these estimates a reasonable assumption to make is that $m_s(1\text{ GeV}) \approx 300$ MeV.

In summary, the input used to solve for the functional form of $m_f(M)$ are Eqs. (6.4b), (6.5b) and (6.6) with $\Lambda = 500$ MeV, $m_s(1\text{ GeV}) = 300$ MeV, and $m_u : m_d : m_s = 1 : 1.8 : 36$ at large M. The result of a numerical calculation is shown in Fig. 8. Above 1 GeV the quark masses decrease slowly with M. Their ratios approach constant values as can readily be seen by inspection of the differential equations. As M decreases below 1 GeV the masses increase rapidly. Notice, though, that when $M > 700$ MeV the up and down quark masses are really very small. The color structure constant is small and decreasing above 1 GeV but increases rapidly below 1 GeV. Evidently a perturbation expansion breaks down somewhere around 1 GeV. More will be said about this in Section 7. These results are very similar to those of Georgi and Politzer.[27] The differences are that we do not consider charm in this paper, although it is clear how to include more quark flavors. Also, the initial values of m_s and α_c are smaller in our paper.

Finally the optimum choice of M must be made. A constant value of M will not do as shown, for example, by Kislinger and Morley[8] and Freedman and McLerran.[14] In higher order in perturbation theory powers of $\log M^2$ appear. For the special case of a one-flavor quark gas with zero quark mass and zero temperature, dimensional analysis implies that the logarithms must be $\log(\mu^2/M^2)$. If M was constant then a perturbation expansion would certainly not converge at large enough μ, at odds with what we expect from asymptotic freedom. If we choose $M^2 = \mu^2$ then contributions from higher orders are minimized. But why should $M^2 = \mu^2$ rather than $M^2 = 4/5\,\mu^2$? The exact coefficient is important if we are to make use of the value of Λ obtained from lepton-hadron scattering as in Eq. (6.8). Furthermore, what is the correct choice of M when there are several flavors with different chemical potentials, non-zero quark masses and a non-zero temperature? Dimensional analysis cannot even fix the function form of M in such a case.

Consider deep-inelastic lepton-hadron collisions. There $M^2 = Q^2$ and the quark mass $m(M^2 = Q^2)$ is the appropriate parton mass.[27] What is the quantity analogous to Q^2 in a very high temperature and/or density many-body system where parton-parton (parton here meaning nearly free quarks or gluons) interactions are almost negligible? One possibility would be to consider parton-parton scattering in the medium. We would do a thermal average over the ingoing momenta and calculate the average four-momentum transfer squared. The objection to this proposal is simply that we cannot carry out the calculation given our present knowledge of QCD. When attempting to do the average there will be a finite interval of integration over the region where the four-momentum transfer is small, hence perturbation theory is inapplicable.

An alternative is to notice that a parton will undergo a large momentum transfer when it makes an elastic collision with the boundary of the system. We argue that M should be chosen as the negative of the square of the four-momentum transferred to the parton by the boundary of the system, appropriately averaged over each parton's thermal momentum distribution and over all partons. More explicitly

$$M^2 = \frac{4}{3} \frac{\sum_i n_i \langle \underset{\sim}{k}^2 \rangle_i}{\sum_j n_j} \tag{6.10}$$

where $\langle k^2 \rangle_i$ is the thermal average of the three-momentum squared of the parton of type i, and n_i is the total number of partons of that type. This argument does not depend on the existence of sharp walls: the boundary may be diffuse. It also does not depend on the frequency of collision of partons with the boundary. If the quarks have non-zero masses then the right side of Eq. (6.10) depends on M through $m_f(M)$, and so Eq. (6.10) is an integral equation for M. For instance, for one flavor of quark at zero temperature

$$M^2 = \frac{4}{5} k_F^2(M) = \frac{4}{5} \left(\mu^2 - m^2(M)\right) .$$

For the purposes of this paper it is sufficient to calculate Eq. (6.10) using the non-interacting gas formulae, but for fourth order one might want to calculate it using the lowest order corrections in α_c.

Although this choice of the subtraction point may seem rather strange at first, it does coincide with our current conception of hadron structure. At short distances inside a hadron the quarks behave as if they were nearly

non-interacting. At large distances the quarks are pulled back in by some collective confining force whose detailed mechanism is not yet understood. In the MIT bag model[10,11] this is achieved by postulating a bag pressure on the surface of the hadron which confines the quarks. The quarks feel very little momentum transfer deep inside the hadron, but feel a strong momentum transfer near the surface. Of course the origin of the boundaries of a hadron and a thermal system may be different but their effect is the same: to confine the particles to some limited volume of space.

It has been shown that the thermodynamic potential for QCD satisfies a renormalization group equation with zero anomalous dimension.[14] Therefore the renormalization group improvement to the perturbative expansion of the thermodynamic potential consists of the replacement of the coupling constant and the masses by ones depending on M, M being determined by Eq. (6.10).

7. NUMERICAL RESULTS AND PHYSICAL INTERPRETATION

A natural scale for separating high- from low-energy density hadronic systems is provided by the average energy density of stable nuclei, $\varepsilon_{SN} \sim 150$ MeV/fm^3. For low energy densities a reasonable description of the system would be obtained by considering it as a gas of free protons, neutrons, deuterons, etc. with small perturbations due to two-body scattering. At high-energy densities there are two prominent competing theories.[31] One approach is to describe the system as a gas of free quarks (and possibly also gluons). This approach appeared in a textbook[31] even before the discovery of asymptotic freedom in quantum chromodynamics. In such a theory, of course, there is no upper limit to the temperature. Although quantum chromodynamics is a very appealing candidate for the strong interactions, it should be pointed out that there is no direct experimental evidence for the existence of a high-energy density macroscopic system of nearly non-interacting quarks and gluons.

In stark contrast is the statistical bootstrap approach due primarily to Hagedorn.[19] The basic idea in this approach is that there are no fundamental hadronic constituents: all hadronic states including resonances are treated on an equal footing. There are an infinite number of such resonances, and they become more and more closely spaced as the mass increases. The asymptotic form of this mass spectrum is

$$\rho(m) \underset{m \to \infty}{\longrightarrow} a m^{-b} \exp(m/T_0) \quad , \tag{7.1}$$

where $T_0 \approx 160$ MeV and the currently (1973) favored value for b is 3. This asymptotic spectrum is strongly suggested by current resonance data

up to several GeV. This exponential rise is also predicted by dual resonance models.[32] Although different versions predict different values of b, they consistently[33] have $T_0 \approx 160 \pm 15$ MeV. The absolute scale in these models is determined by the Regge slope parameter, $\alpha' \approx 1$ GeV^2.

The Hagedorn description of hadronic matter then is to treat each species of hadron (stable as well as resonance) as a non-interacting gas with some temperature and chemical potential. The calculation of thermodynamic quantities, such as the partition function Z, will involve an integration over $\rho(m)dm$. This integral will not converge unless the temperature T is less than T_0. Hence T_0 is a limiting temperature for hadronic matter. In fact, high-energy hadron-hadron collisions provide strong evidence[19] for a limiting temperature of ~160 MeV, although one must introduce various unknown functions with associated parameters to deal with the dynamics of the collision (roughly the distribution of thermal sources).

Finally the connection between Hagedorn's statistical analysis and the dual resonance models, along with other points, has been extensively discussed by Frautschi.[34] It should not be surprising that the dual resonance models lead to a maximum temperature since they assume that hadron dynamics is dominated by resonances.

Thus there appears to be a problem. The Hagedorn description of hadronic matter, which has some strong experimental support, is characterized by a limiting temperature. The free quark and gluon description of dense matter, which also has strong but indirect experimental support in the form of asymptotic freedom (or scaling), has no limiting temperature. How can these two different views be reconciled, if at all?

A partial solution to this problem was suggested in the original MIT bag model paper.[10] In a simplified version of that model, with all particles massless and a zero coupling constant, it was shown that the hadronic mass spectrum grows as $\sim\exp(m/T_0)$ where T_0 is calculable and has a unique interpretation as the temperature of the system. We shall now go through a rather similar but more general argument which suggests that the same result occurs in quantum chromodynamics.

Consider the thermodynamic relation

$$E = -PV + TS + \underset{\sim}{\mu} \cdot \underset{\sim}{N} \quad . \tag{7.2}$$

Here E is the total energy of the system, V the volume, S the entropy, and $\underset{\sim}{\mu}$ determines the average baryon number, charge, strangeness, etc. In quantum chromodynamics we know that the equation of state tends toward that of a free gas at high temperature or density because of asymptotic freedom. Hence $P > 0$ for large T or $|\underset{\sim}{\mu}|$. Conversely, if quantum chromodynamics binds quarks and gluons into hadrons at large distances, then at low enough T and $|\underset{\sim}{\mu}|$, $P < 0$. We shall assume that this is the case. Of course the proof is one of the major outstanding problems in theoretical physics! A consequence of this assumption is that there exists a set of T_c, $\underset{\sim}{\mu}_c$ such that $P(T_c, \underset{\sim}{\mu}_c) = 0$. At these critical points

$$S = (E - \underset{\sim}{\mu}_c \cdot \underset{\sim}{N}) / T_c \quad , \tag{7.3}$$

and so the level density of the system is

$$\text{level density} \sim \exp[(E - \underset{\sim}{\mu}_c \cdot N) / T_c] \quad . \tag{7.4}$$

For a system with a given set of conserved quantum numbers the level

density rises exponentially as energy is fed into the system. Furthermore, if the total energy is held fixed as well, then the system is in mechanical equilibrium and hence is a metastable state. This follows because a contraction leads to $P > 0$ while an expansion leads to $P < 0$. Most likely the system will be unstable with respect to hadron emission however. Thus we interpret this system as a high mass hadronic resonant state. Quantum chromodynamics then predicts an asymptotic mass spectrum of the form of Eq. (7.1). The exponent b in that equation cannot be determined by this thermodynamic argument because it corresponds to a $\log V$ term in S and such terms are always thrown away in thermodynamic calculations; $(\log V)/V \to 0$.

The assumptions we made above are worth emphasizing. The first was that at sufficiently low energy densities the pressure was negative. This may be interpreted as the confinement of quarks and gluons to the interior of hadrons. This led to the mechanical stability of the system and the exponential rise of the level density. We also assumed that these many-body systems corresponded to asymptotically heavy hadronic resonances. Of course this is a valid assumption only if the resonances are not bounded in spatial extent.

A very similar situation has been considered recently by Polyakov[35] and Susskind[36] in the context of lattice gauge theories. Quantum chromodynamics on a lattice has the property of confinement. They show, however, that at high temperatures the color charge is Debye screened and confinement is spoiled. Thus there is a hadron phase at low temperature and a free quark phase at high temperature. In fact there is a sharp transition between the confined and unconfined phases. Unfortunately the continuum limit of lattice field theories is not understood.

Even if quantum chromodynamics has an exponentially rising level density at some critical points, there can still be differences between its predictions and those of a Hagedorn statistical bootstrap type of thermodynamics. For the latter with zero net quantum number densities it is found that[33]

$$\varepsilon \sim \begin{cases} (T - T_0)^{b - 7/2} & b < 7/2 \\ \log(T_0 - T) & b = 7/2 \\ \text{constant} & b > 7/2 \end{cases} \tag{7.5}$$

as $T \to T_0$. The behavior of P is the same except that b is replaced with $b + 1$. What we would expect physically is that the system will be in the quark phase above a critical energy density $\varepsilon_c(T_c, \underset{\sim}{\mu}_c)$ and in the hadron phase below it. Naively this means that if the energy density is high enough then the hadrons overlap so strongly that the quarks forget which hadron they belong to and so can travel long distances in the system. The transition energy density should be characterized by that of a proton. Thus there appears to be a definite mismatch of these two approaches if $b \leqslant 7/2$, but probably not if $b > 7/2$. $b > 7/2$ then is our preferred value. It should be noted that the primary reason for choosing $b \leqslant 7/2$ originally was that if b were otherwise, then above a certain energy density thermodynamic equilibrium could not be maintained. If there is a transition from hadronic matter to quark-gluon matter then thermodynamic equilibrium can be maintained at all energy densities.

Let us begin our numerical investigation by considering the MIT bag model predictions for the pressure. The bag model parameters are determined by fitting the low lying hadron masses.[11] The confining bag

pressure is $B = (145\ \text{MeV})^4$, and the quark masses are $m_s = 280$ MeV, $m_u = m_d = 0$. The quark-quark interaction is calculated to order $\alpha_c = 0.55$. Using these parameters in Eqs. (3.23), (3.31), (3.32), (3.33) and (4.16), and assuming zero net baryon number, charge and strangeness, we obtain the curves shown in Fig. 9. The odd choice of scale was necessary because the pressure goes through zero. $P_{(0)}$, $P_{(2)}$, and $P_{(3)}$ denote the contributions from order 1, α_c and $\alpha_c^{3/2}$, respectively. $P_{(0)} - B$ is negative below T = 100 MeV, $P_{(0)} + P_{(2)} + P_{(3)} - B$ is negative below T = 75 MeV. There are two interesting points to notice. The first is that, in this model which includes the effects of confinement, the pressure is negative below some critical temperature and positive above it. This is what we expect. The second point is that the expansion does not really seem to converge very well. That is, at temperatures above 50 MeV the result depends crucially on how many terms in the expansion we keep. Evidently $\alpha_c = 0.55$ is too large for a fast convergence at high temperature. In fact it may not converge at all. In all fairness we must remember that α_c was determined at a subtraction point of ~1 GeV. That is, the bag model does not employ the renormalization group since there is not much variation in the average subtraction point among the low lying hadrons.

Next let us consider the predictions of quantum chromodynamics. The coupling constant α_c is now the renormalization group running coupling constant depending on T and $\underset{\sim}{\mu}$. The quark masses m_u, m_d and m_s also depend on T and $\underset{\sim}{\mu}$. These functions were discussed in Section 6. Using these functions in Eqs. (3.23), (3.31), (3.32), (3.33) and (4.16), and assuming zero net baryon number, charge and strangeness, we obtain the curves shown in Fig. 10. To facilitate comparison, the scale and notation is identical

to Fig. 9, except that perturbative quantum chromodynamics has no bag pressure of course. There are a number of interesting points about this graph. Due to asymptotic freedom the expansion seems to be converging very well at high temperature. In fact, keeping just the first three terms seems to be enough above about $T \approx 500$ MeV. When $\underset{\sim}{\mu} = 0$, the subtraction point $M \approx 4T$. Thus the expansion converges rapidly when $\alpha_c \lesssim 0.1$, corresponding to $g^2/4\pi \lesssim 0.4$. However, when T is reduced to 230 MeV then $P_{(3)} \simeq -P_{(2)} \simeq P_{(0)}$ and so the first three terms cannot be expected to yield a good approximation to the true answer. This corresponds to $\alpha_c \gtrsim 0.3$ or $g^2/4\pi \gtrsim 1.2$. One might expect that by keeping more terms in the expansion of $P = -\Omega$ and by solving the renormalization group equation to higher order in α_c, the temperature above which a perturbative expansion is valid could be pushed down. Certainly there is no obvious way of deciding upon the radius of convergence of the expansion within our calculational framework. At lower temperatures one must worry about the mechanism of confinement, which is a long range nonperturbative phenomenon. Also our choice of subtraction point will no longer be valid if the quarks and gluons are clustering into hadrons. It seems unlikely, therefore, that one could prove that the pressure becomes negative in the framework of perturbation theory. That this is an important problem was discussed earlier in this section. The best we can do is to say that the strong coupling of quarks and gluons probably results in their confinement to hadrons at temperatures of order $T \approx 200 \pm 100$ MeV. The question of a phase transition cannot be properly addressed.

A question that can be asked is: How does P vs. T look at fixed nonzero chemical potential? The most interesting case is that with

$\mu_u = u_d \equiv \mu$, $u_s = 0$, which corresponds to the quantum numbers of nuclear matter. For μ not too large, the pressure curves are very similar to those of Fig. 10 except that they are shifted to the left. The greater μ is the greater the shift is. To get a semiquantitative estimate of the T and μ dependence of the transition point or radius of convergence, it is convenient to pick the minimum of the $P_{(0)} + P_{(2)} + P_{(3)}$ curve as the characteristic point. The T-μ dependence is plotted in Fig. 11. Above $\mu = 600$ MeV the dip in the P vs. T curve is flattening out, making it difficult to pinpoint the minimum. All along the solid line in Fig. 11 the subtraction point is consistently at 720 MeV. The dashed line is an extension with the same subtraction point. Above the line a reasonable description of the many-body system should consist of a basis set of free quark and gluon states with some perturbative interactions superimposed. Below the line a reasonable description of the system should consist of a basis set of free hadron states with some perturbative interactions superimposed. It is amusing that $\alpha_c(M = 720 \text{ MeV}) = 0.53$ which is very close to the MIT bag model value.

It is interesting to consider the baryon number density and energy density dependence of the transition temperature. The baryon number density, entropy density, and energy density are

$$n_B = \frac{1}{3}\left(\frac{\partial P}{\partial \mu}\right)_T ,$$

$$\mathcal{S} = T\left(\frac{\partial P}{\partial T}\right)_\mu , \qquad (7.6)$$

$$\varepsilon = -P + T\mathcal{S} + 3\mu n_B .$$

Although we expect the minimum in the pressure curve to correspond more or less to the transition point, we cannot evaluate n_B and ε with any reliability using the same curve. For instance, the entropy is zero at the minimum! Again, to get a crude semiquantiative estimate, let us evaluate n_B and ε using the noninteracting gas formulae with the quark masses evaluated at $M = 720$ MeV. In Fig. 12 we plot T_c vs. n_B and in Fig. 13 we plot T_c vs. ε. Above the lines we expect the system to be in the quark-gluon phase, and below the line we expect the system to be in the hadron phase. To get a feeling for the numbers, a proton has a charge radius of 0.8 fm yielding an average baryon number density of 0.5 fm^{-3} and an average energy density of 0.5 GeV fm^{-3}. However, a hard core of radius 0.2 fm containing one-third of the charge and energy results in a baryon number density of 10 fm^{-3} and an energy density of 10 GeV fm^{-3}.

We can draw a parametric curve relating ε and n_B at the transition point with T_c being the parameter. This is shown in Fig. 14. Again the quark phase lies above the line and the hadron phase below it. One might wonder whether matter could be formed in the quark phase in the laboratory. Clearly the best chance to form such matter is to collide two heavy nuclei at high energy in order to reach the high energy densities required. To get a crude estimate of the densities attainable, suppose that two equal mass nuclei collide at near zero impact parameter. Assume that they stop each other within one Lorentz contracted volume in the center of mass. Then one can trivially calculate the ε vs. n_B curve which is parametrized by the individual beam kinetic energy per nucleon in a colliding beam machine. This is the dashed curve in Fig. 14. Note

that somewhere around 1.5 GeV/nucleon a transition from hadron matter to quark matter is possible. Beam energies well above this should be feasible with present day technology. The heaviest nucleus available, say ^{238}U, should be used to obtain the maximum possible stopping power. An important point to notice is that the quark-gluon matter will probably be formed in a highly excited state, i.e. large T rather than $T = 0$. This is because

$$n_B \sim \text{beam energy} \quad ,$$

whereas

$$\varepsilon \sim (\text{beam energy})^2 \quad .$$

Of course these conclusions are based on a number of semiquantitative results. Nevertheless these crude estimates are highly suggestive.

The equation of state is a graph of P vs. ε at fixed T. This is shown in Fig. 15 using $P = P_{(0)} + P_{(2)} + P_{(3)}$ and Eq. (7.2). For $T \gtrsim 500$ MeV the difference between the equation of state including interactions and the curve $P = 1/3\,\varepsilon$ is inconsequential. On a given isotherm, μ increases as we go up the curve. Hence M increases, α_c decreases, and P approaches $1/3\,\varepsilon$ ever more closely.

8. SUMMARY AND TOPICS FOR FUTURE INVESTIGATION

In this paper we calculated the thermodynamic potential for quantum chromodynamics to orders 1, α_c, and $\alpha_c^{3/2}$. The number of quark flavors, the chemical potentials, and the quark masses were left arbitrary while the temperature was kept nonzero. The renormalization group was used to improve the expansion by allowing α_c and the quark masses to be functions of the temperature and chemical potentials. Numerical calculations were presented and the onset of the breakdown of the expansion was investigated. Based on a variety of evidence we argued that this breakdown corresponds to a phase transition from matter which is most easily described in terms of quarks and gluons to matter which is most easily described in terms of hadrons. What topics for future investigation are suggested by this work?

The most obvious extension is to calculate the order α_c^2 term. The calculation will be much more difficult than the α_c and $\alpha_c^{3/2}$ calculations. First of all, the question of Landau gauge vs. Feynman gauge must be tackled directly for the first time, as discussed in Section 5. Secondly, a typical diagram in order α_c has eight individual algebraic terms associated with it, while a typical diagram in order α_c^2 has sixty-four individual terms. Thirdly, the finite values of the quark masses, especially m_s, complicates the formulae to a greater degree than in lower orders. We cannot neglect m_s in comparison with T because the interesting region to investigate is precisely the region where $T \approx m_s$. One must calculate the β_g and γ_m functions of the renormalization group to the next highest order with nonzero masses. This has not yet been done. Also, nonzero masses mean that the pressure in order α_c^2 involves

numerically integrating six-dimensional integrals as opposed to three in lower orders. Finally, consistency for the subtraction point demands that the three momentum squared of the particles in the system must be computed to order α_c as discussed in Section 6. It is not clear whether the effort involved in computing the order α_c correction is worthwhile when one considers that the next term in the expansion is of order $\alpha_c^{5/2}$.

A major contribution would be just an existence proof that the pressure in quantum chromodynamics does go negative at sufficiently low temperature and baryon number density. Undoubtably such a proof would involve a more powerful technique than the perturbation theory we have been using. Freedman and McLerran[14] noticed an interesting property that could be useful in this context. That is, if the thermodynamic potential is regarded as a functional of the full propagators and vertices, then independent variations of these propagators and vertices show that the thermodynamic potential is at a stationary point. This means that a variational construction of the thermodynamic potential is possible.

There is an interesting calculation which is one step removed from quantum chromodynamics but which nevertheless would be very instructive. Solve the equations in the cavity approximation to the MIT bag model with an arbitrary number of quarks having arbitrary masses and with $\alpha_c = 0$. Use these wave functions as input to calculate statistically the level density of the system. This would give us, in this simple model at least, the function multiplying $\exp(E/T_c)$ [see Eq. (7.1)]. This has been done only for scalar particles in a two-dimensional bag.[10]

A topic which has not been investigated at finite or zero temperature is correlations. If the temperature or baryon number density is high

then the correlation functions may be calculated perturbatively. It will be interesting to learn how quark-quark correlations compare with quark-antiquark correlations, for example. It is not clear whether a perturbative calculation will tend to cluster quarks in the expected manner. A closely related topic is to calculate the local color fluctuations in the system.

If one is interested in studying the transition from quark-gluon matter to hadron matter then the problem of nonperturbative solutions and confinement must eventually be faced. This problem is far more difficult than the others mentioned so far. The relevance of instantons in many-body calculations has been pointed out by Harrington and Shepard.[37] Instantons are nonperturbative solutions which give significant contributions when the coupling takes on moderate values, of order slightly less than unity say. If large values of the coupling are necessary to describe confinement near the transition region then presumably a strong coupling expansion will have to be developed.

One may ask the question: Is there a remnant of nonperturbative confinement effects at high temperature and density? The answer seems to be yes. One step in the renormalization scheme is to subtract off the vacuum piece of Ω. Schematically

$$\Omega_R^I(T,\underset{\sim}{\mu}) = \Omega^I(T,\underset{\sim}{\mu}) - \Omega^I_{\substack{\text{norm}\\ \text{vac}}}$$

where the normal vacuum is constructed perturbatively,

$$\Omega^I_{\substack{\text{norm}\\ \text{vac}}} = \lim_{\substack{T\to 0\\ \mu\to 0}} \Omega^I(T,\underset{\sim}{\mu}) \quad .$$

If there is a lower state constructed nonperturbatively which represents the true vacuum, then we should have

$$\Omega_R^I(T,\underset{\sim}{\mu}) = \Omega^I(T,\underset{\sim}{\mu}) - \Omega^I_{\substack{\text{true}\\ \text{vac}}}$$

The difference between these two prescriptions amounts to an additive constant to the thermodynamic potential. This may be the origin of the bag model confining-pressure B.

Finally there is the problem of finding an experimental signature for the production of high temperature quark-gluon matter in high-energy heavy-ion collisions. Probably this question cannot be considered separately of the dynamics of the collision.

We conclude that there is much work still to be done. Some of these and other problems are currently being investigated.

I am grateful to S. Chin for pointing out several corrections to the original manuscript.

REFERENCES

1. H.D.Politzer, Phys. Rep. 14C, 129 (1974).
2. L.Dolan and R.Jackiw, Phys. Rev. D9, 3320 (1974).
3. S.Weinberg, Phys. Rev. D9, 3357 (1974).
4. J.C.Collins and M.J.Perry, Phys. Rev. Lett. 34, 1353 (1975).
5. G.Baym and S.A.Chin, Phys. Lett. 62B, 241 (1976).
6. G.Chapline and M.Nauenberg, Nature 264, 235 (1976).
7. B.A.Freedman and L.D.McLerran, MIT Report No. 541 (1976)(unpublished).
8. M.B.Kislinger and P.D.Morley, Phys. Lett. 67B, 371 (1977).
9. G.Chapline and M.Nauenberg, Phys. Rev. D16, 450 (1977).
10. A.Chodos, R.L.Jaffe, K.Johnson, C.B.Thorn, and V.F.Weisskopf, Phys. Rev. D9, 3471 (1974).
11. T.DeGrand, R.L.Jaffe, K.Johnson, and J.Kiskis, Phys. Rev. D12, 2060 (1975).
12. C.Bernard, Phys. Rev. D9, 3312 (1974).
13. M.B.Kislinger and P.D.Morley, Phys. Rev. D13, 2771 (1976).
14. B.A.Freedman and L.D.McLerran, Phys. Rev. D16, 1130, 1147, 1169 (1977).
15. P.D.Morley, Phys. Rev. D17, 598 (1978).
16. V.Baluni, Phys. Rev. D17, 2092 (1978).
17. M.B.Kislinger and P.D.Morley, Ap. J. 219, 1017 (1978).
18. I.A.Akhiezer and S.V.Peletminski, J. Exptl. Theor. Phys. 38, 1829 (1960) [Soviet Physics JETP 11, 1316 (1960)].
19. R.Hagedorn, Nuovo Cimento Suppl. 3, 147 (1965); ibid, 6, 311 (1968); Nuovo Cimento 52A, 1336 (1967); ibid, 56A, 1027 (1968); Astron. and Astrophys. 5, 184 (1970); in Cargèse Lectures in Physics, edited by E.Schatzmann, Vol. VI (Gordon and Breach, New York, 1973);

R.Hagedorn and J.Ranft, Nuovo Cimento Suppl. 6, 169 (1968).

20. R.P.Feynman, Phys. Rev. 91, 1291 (1953).

21. R.P.Feynman and A.R.Hibbs, Quantum Mechanics and Path Integrals (McGraw-Hill, New York, 1965).

22. L.D.Faddeev, Teor. Math. Fiz. 1, 3 (1970) [Theor. Math. Phys. 1, 1 (1970)].

23. L.D.Faddeev and V.N.Popov, Phys. Lett. 25B, 29 (1967).

24. L.B.W.Jolley, Summation of Series (Dover, New York, 1961), second edition, p.154.

25. R.E.Norton and J.M.Cornwall, Ann. Phys. 91, 106 (1975).

26. M.B.Kislinger and P.D.Morley, Phys. Rev. D13, 2765 (1976).

27. H.Georgi and H.D.Politzer, Phys. Rev. D14, 1829 (1976).

28. H.D.Politzer, Nucl. Phys. B117, 397 (1976).

29. G.C.Fox, Nucl. Phys. B131, 107 (1977).

30. S.Weinberg, in A Festschrift for I. I. Rabi, edited by Lloyd Motz (New York Academy of Sciences, New York, 1977).

31. S.Weinberg, Gravitation and Cosmology (Wiley, New York, 1972).

32. S.Fubini and G.Veneziano, Nuovo Cimento 64A, 811 (1969); K.Bardakci and S.Mandelstam, Phys. Rev. 184 ,1640 (1969); S.Fubini, D.Gordon and G.Veneziano, Phys. Lett. 29B, 679 (1969).

33. K.Huang and S.Weinberg, Phys. Rev. Lett. 25, 895 (1970).

34. S.Frautschi, Phys. Rev. D11, 2821 (1971).

35. A.M.Polyakov, Phys. Lett. 72B, 477 (1978).

36. L.Susskind, SLAC-PUB-2070 (1978).

37. B.Harrington and H.Shepard, Nucl. Phys. B124, 409 (1977); Phys. Rev. D17, 2122 (1978).

FIGURE CAPTIONS

Fig. 1. Bare propagators and vertices in quantum chromodynamics.

Fig. 2. Contour C appearing in Eq. (2.8).

Fig. 3. The second order fermion loop contributions to the thermodynamic potential.

Fig. 4. The second order ghost loop contributions to the thermodynamic potential.

Fig. 5. The second order pure gluon contributions to the thermodynamic potential.

Fig. 6. The gluon correlation contribution to the thermodynamic potential.

Fig. 7. Additional fourth order contributions to the thermodynamic potential not contained in Fig. 6. For simplicity only the bare diagrams are shown.

Fig. 8. Masses of the up, down, and strange quarks and the coupling constant for color SU(3) as functions of the subtraction point.

Fig. 9. The pressure plotted as a function of temperature at zero baryon number density in the MIT bag model of confinement. Note the oscillations as the α_c and $\alpha_c^{3/2}$ terms are added on.

Fig. 10. The pressure plotted as a function of temperature at zero baryon number density in quantum chromodynamics. Note the convergence of the expansion at high temperature.

Fig. 11. Semiquantitative estimate of the temperature and chemical potential dependence of the transition point.

Fig. 12. Semiquantitative estimate of the baryon number density dependence of the transition temperature.

Fig. 13. Semiquantitative estimate of the energy density dependence of the transition temperature.

Fig. 14. Semiquantitative estimate of the energy density vs. baryon number density at the transition point parameterized by the temperature. The dashed curve is an estimate of the densities attainable by colliding two heavy nuclei. The curve is parameterized by the kinetic energy per nucleon per beam of a colliding beam machine.

Fig. 15. Equation of state calculated from $P = P_{(0)} + P_{(2)} + P_{(3)}$.

Fermion

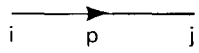

$$S_o = \frac{-\delta ij}{\not{p} - m}$$

Ghost

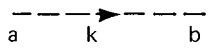

$$W_o = \frac{-\delta ab}{k^2}$$

Gluon

$$D_o = \frac{\delta ab}{k^2} \left[g_{\mu\nu} - (1 - \alpha) \frac{k_\mu k_\nu}{k^2} \right]$$

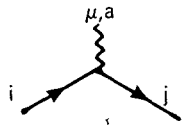

$$\Gamma_o^F = -g\gamma^\mu \tau^a_{ij}$$

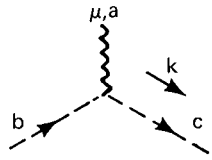

$$\Gamma_o^G = -igf_{abc}k_\mu$$

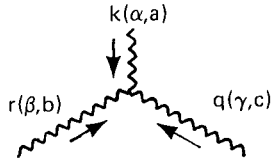

$$\Gamma^V_{o(3)} = -igf_{abc} \left[g_{\beta\gamma} (r - q)_\alpha + g_{\alpha\beta} (k - r)_\gamma + g_{\gamma\alpha} (q - k)_\beta \right]$$

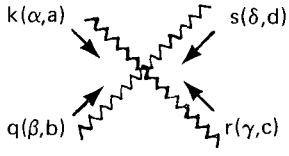

$$\Gamma^V_{o(4)} = -g^2 \left[f_{ade} f_{ebc} (g_{\alpha\beta} g_{\delta\gamma} - g_{\alpha\gamma} g_{\delta\beta}) + f_{abe} f_{edc} (g_{\alpha\delta} g_{\beta\gamma} - g_{\alpha\gamma} g_{\delta\beta}) + f_{ace} f_{edb} (g_{\alpha\delta} g_{\beta\gamma} - g_{\alpha\beta} g_{\delta\gamma}) \right]$$

XBL 786-1143

Fig. 1

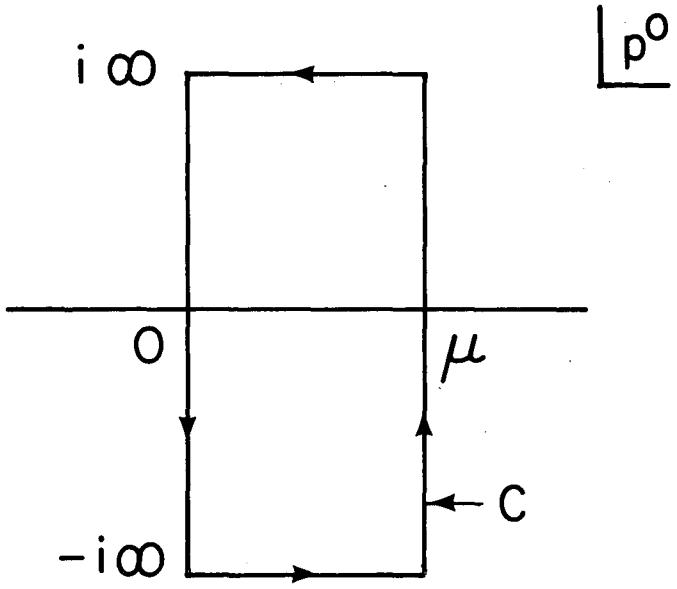

XBL786-1138

Fig. 2

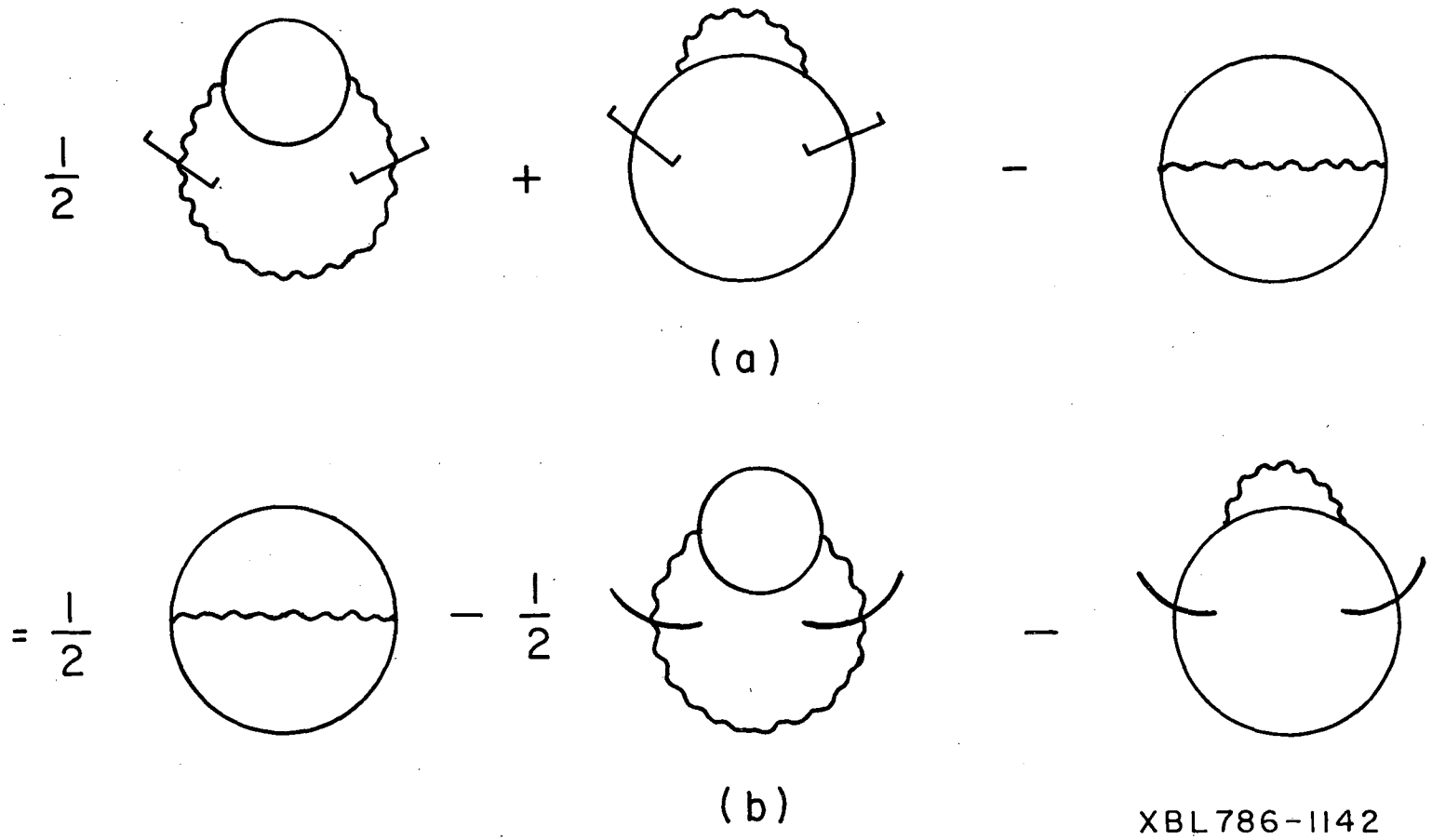

Fig. 3

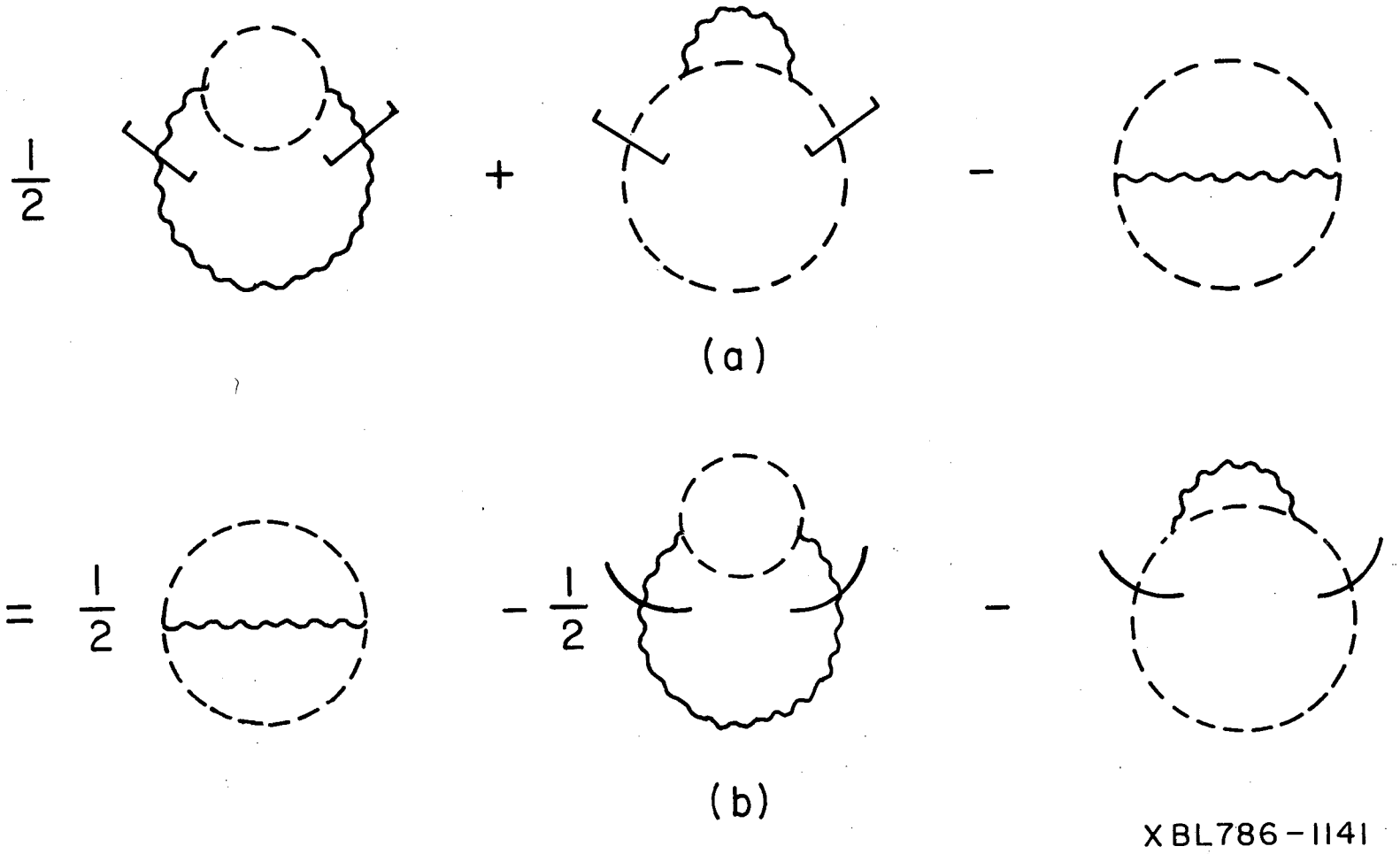

Fig. 4

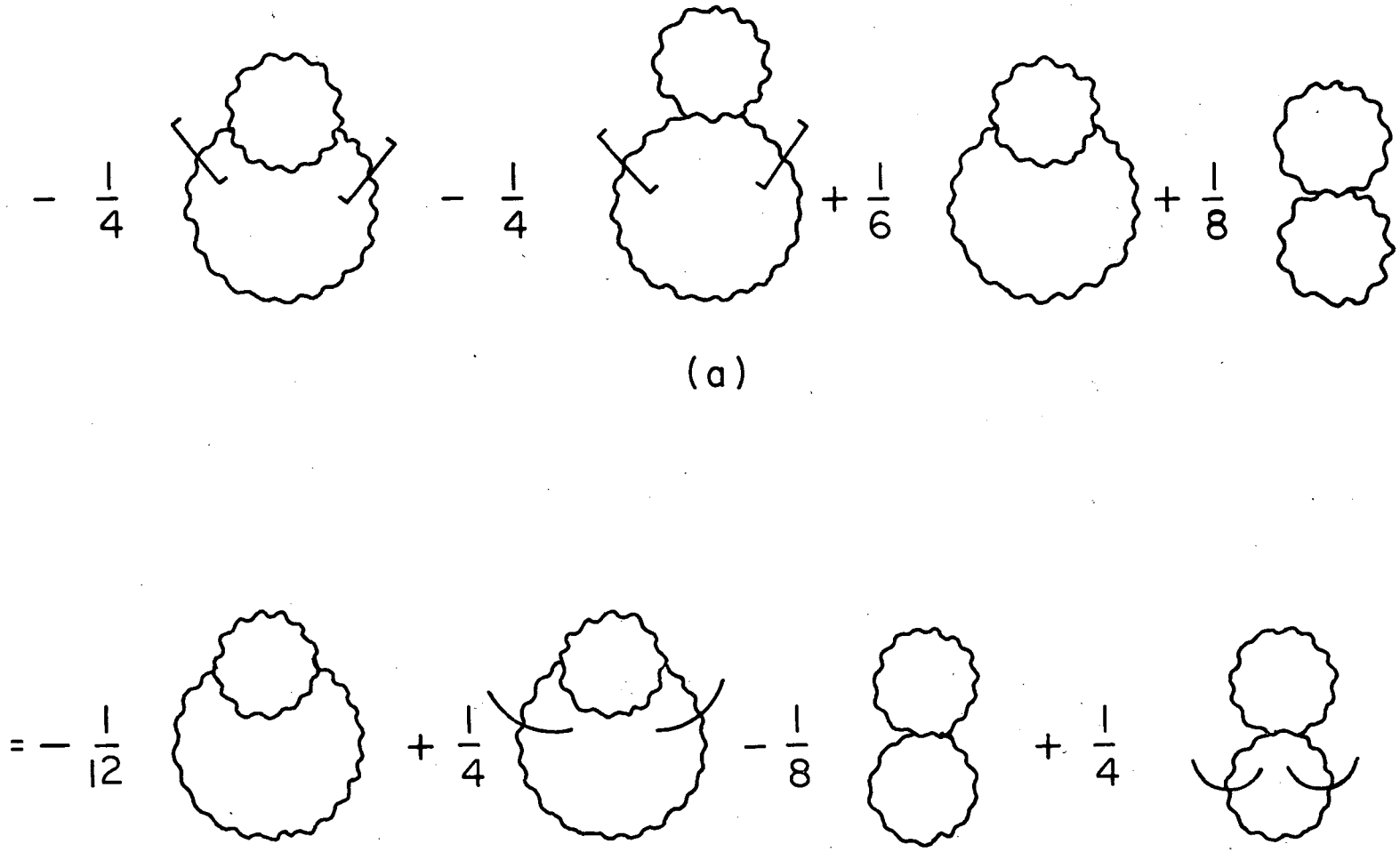
$-\frac{1}{4}$
$-\frac{1}{4}$
$+\frac{1}{6}$
$+\frac{1}{8}$
(a)
$=-\frac{1}{12}$
$+\frac{1}{4}$
$-\frac{1}{8}$
$+\frac{1}{4}$
XBL786-1140

Fig. 5

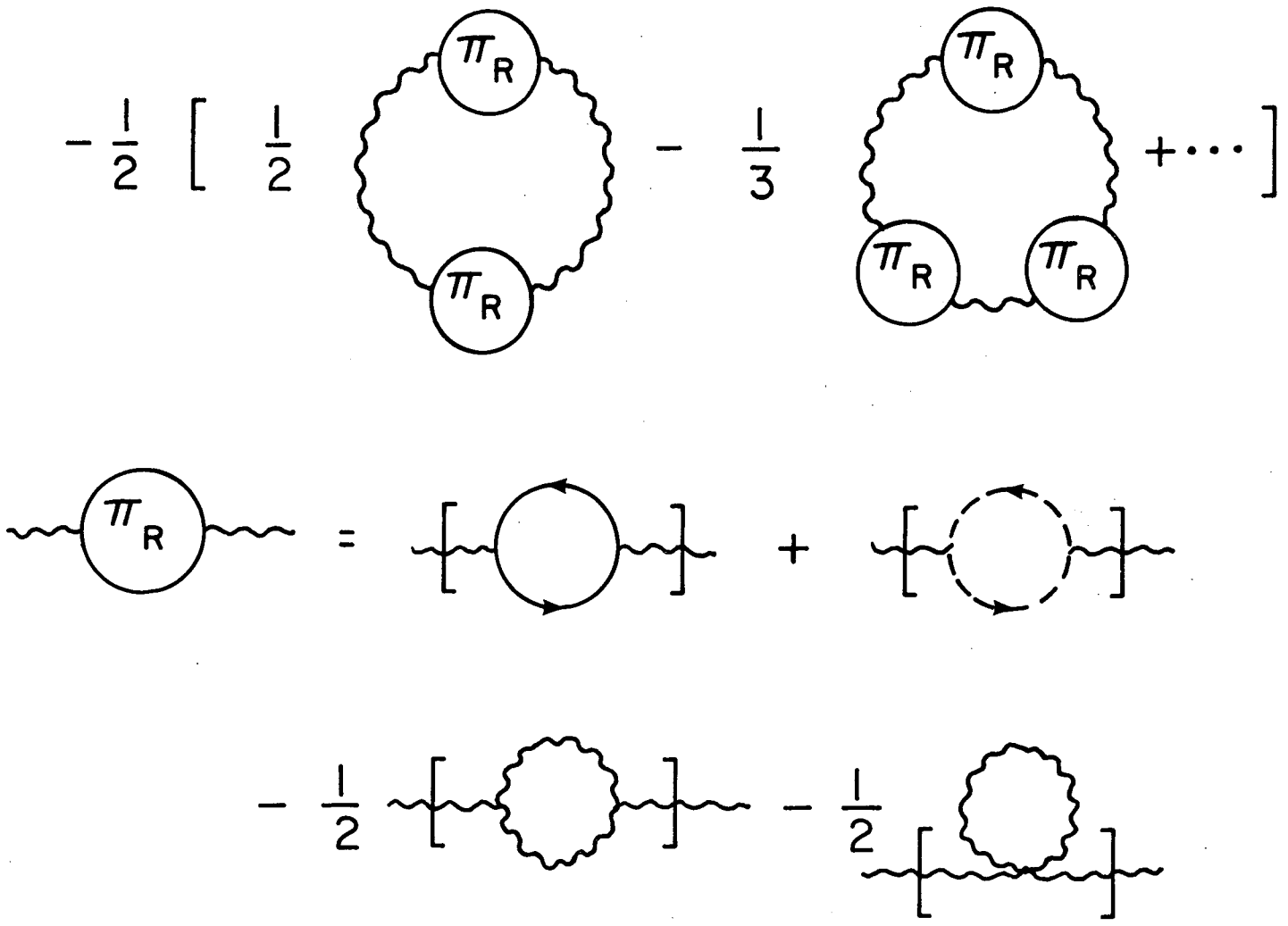

XBL786-1139

Fig. 6

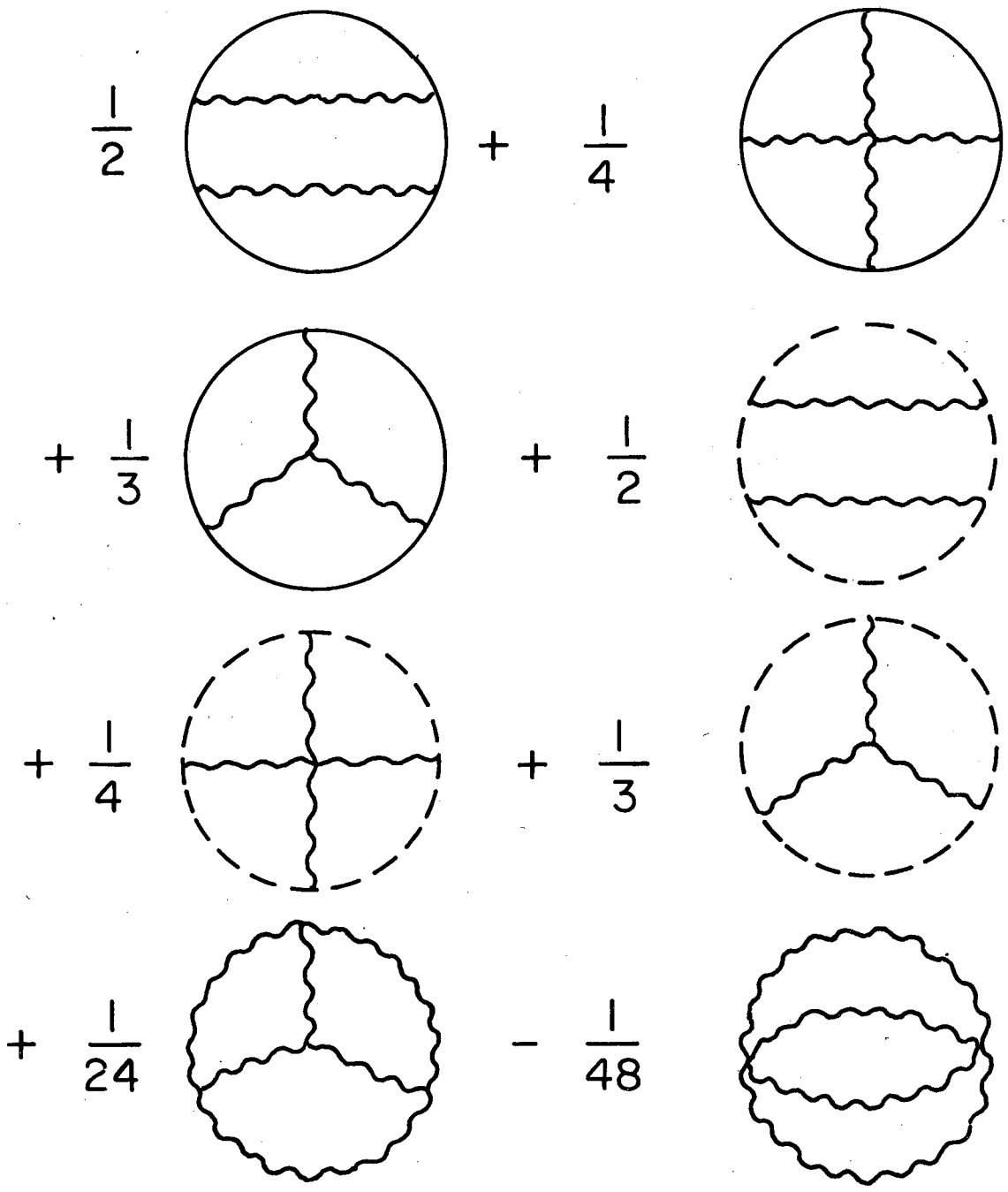

XBL786-1137

Fig. 7

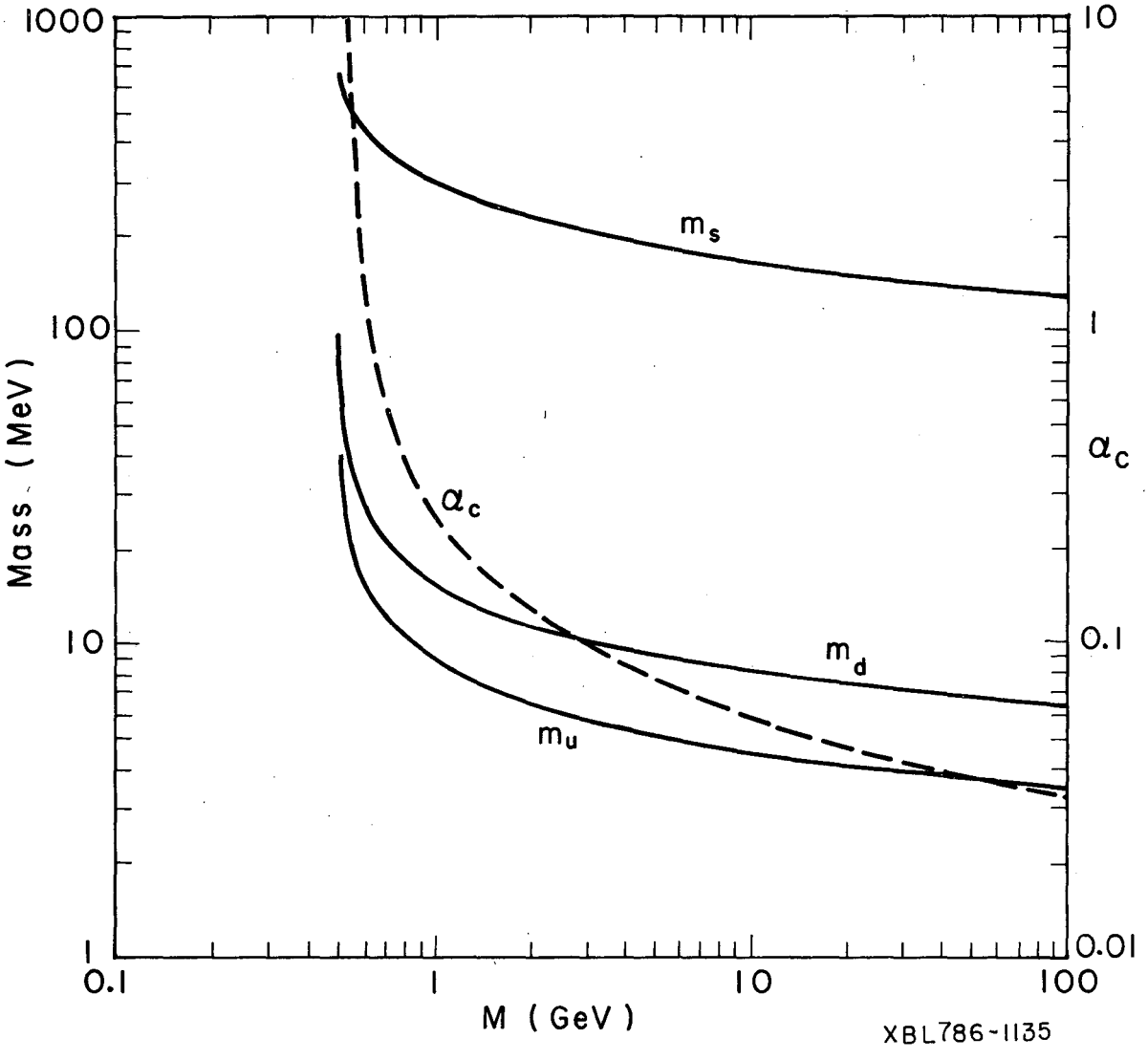
1000
100
10
1
Mass (MeV)
10
1
0.1
0.01
α_c
m_s
m_d
m_u
α_c
0.1
1
10
100
M (GeV)
XBL786-1135

Fig. 8

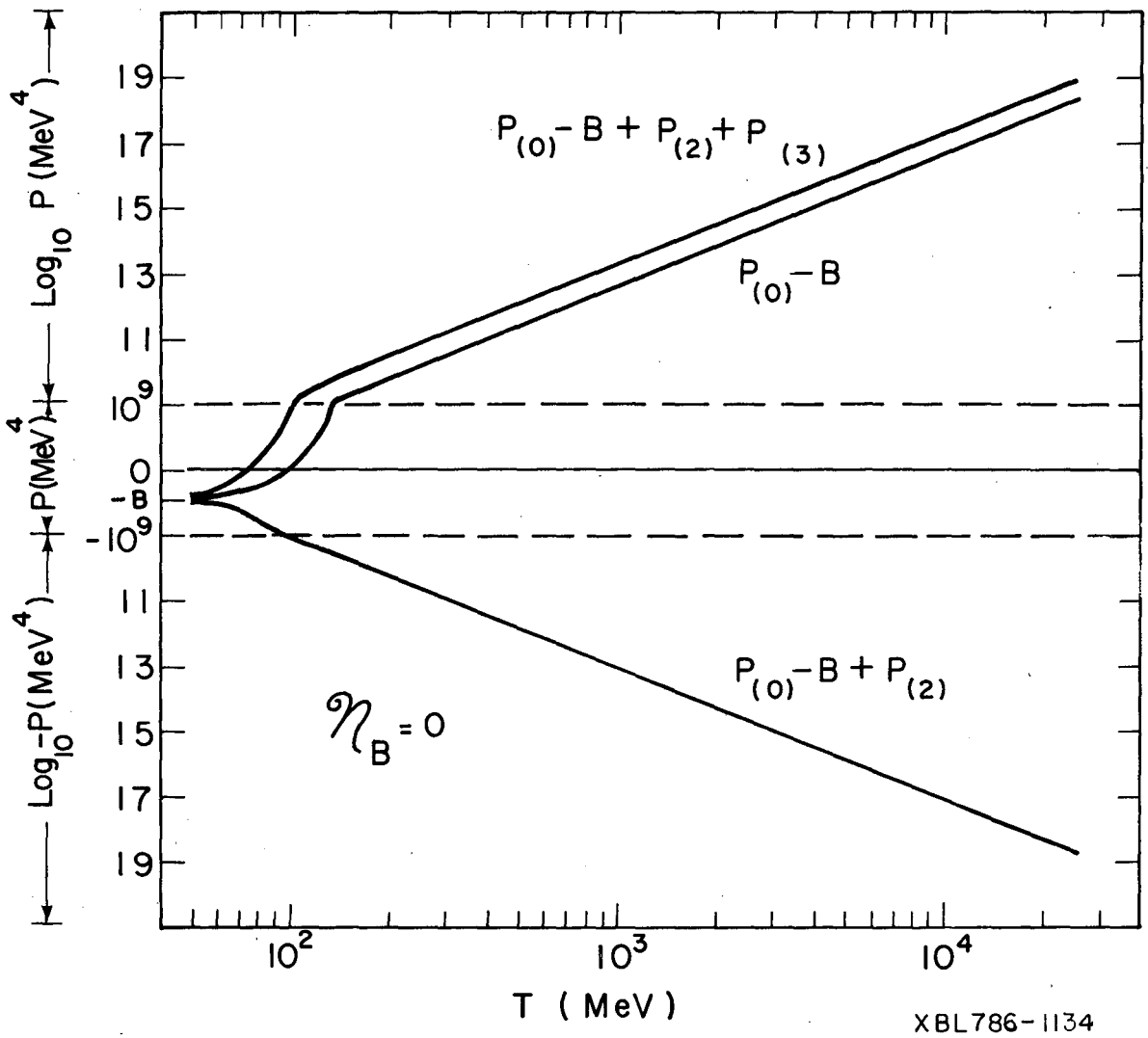
Log10 P (MeV4)
P(MeV4)
Log10 -P(MeV4)
19
17
15
13
11
10^9
0
-B
-10^9
11
13
15
17
19
P(0)-B + P(2)+ P(3)
P(0)-B
P(0)-B + P(2)
ℳB = 0
10^2
10^3
10^4
T (MeV)
XBL786-1134

Fig. 9

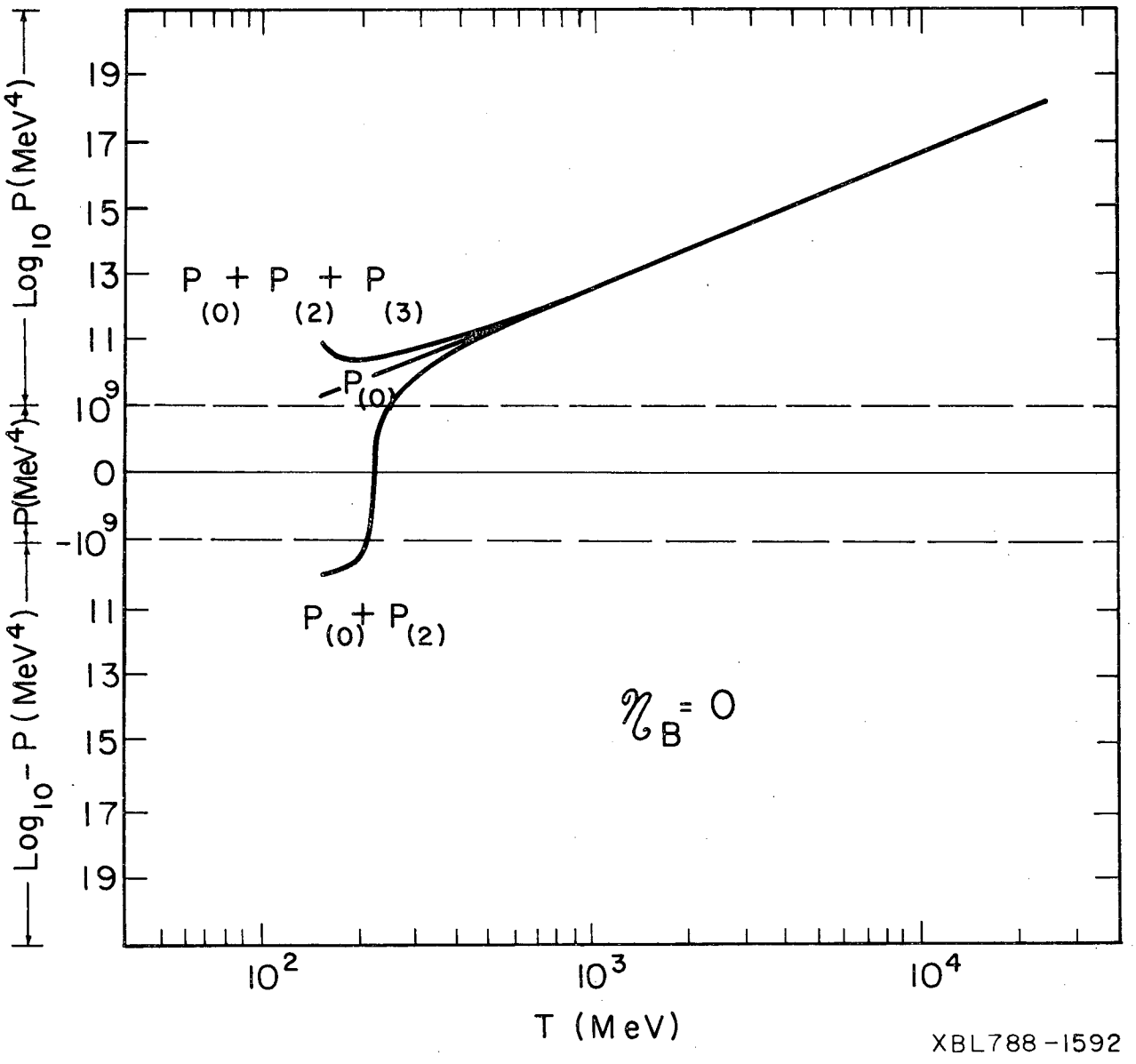
Log10 P (MeV4)
P(MeV4)
Log10 - P (MeV4)
19
17
15
13
11
10^9
0
-10^9
11
13
15
17
19
P (0) + P (2) + P (3)
P (0)
P (0) + P (2)
ηB = 0
10^2
10^3
10^4
T (MeV)
XBL788-1592

Fig. 10

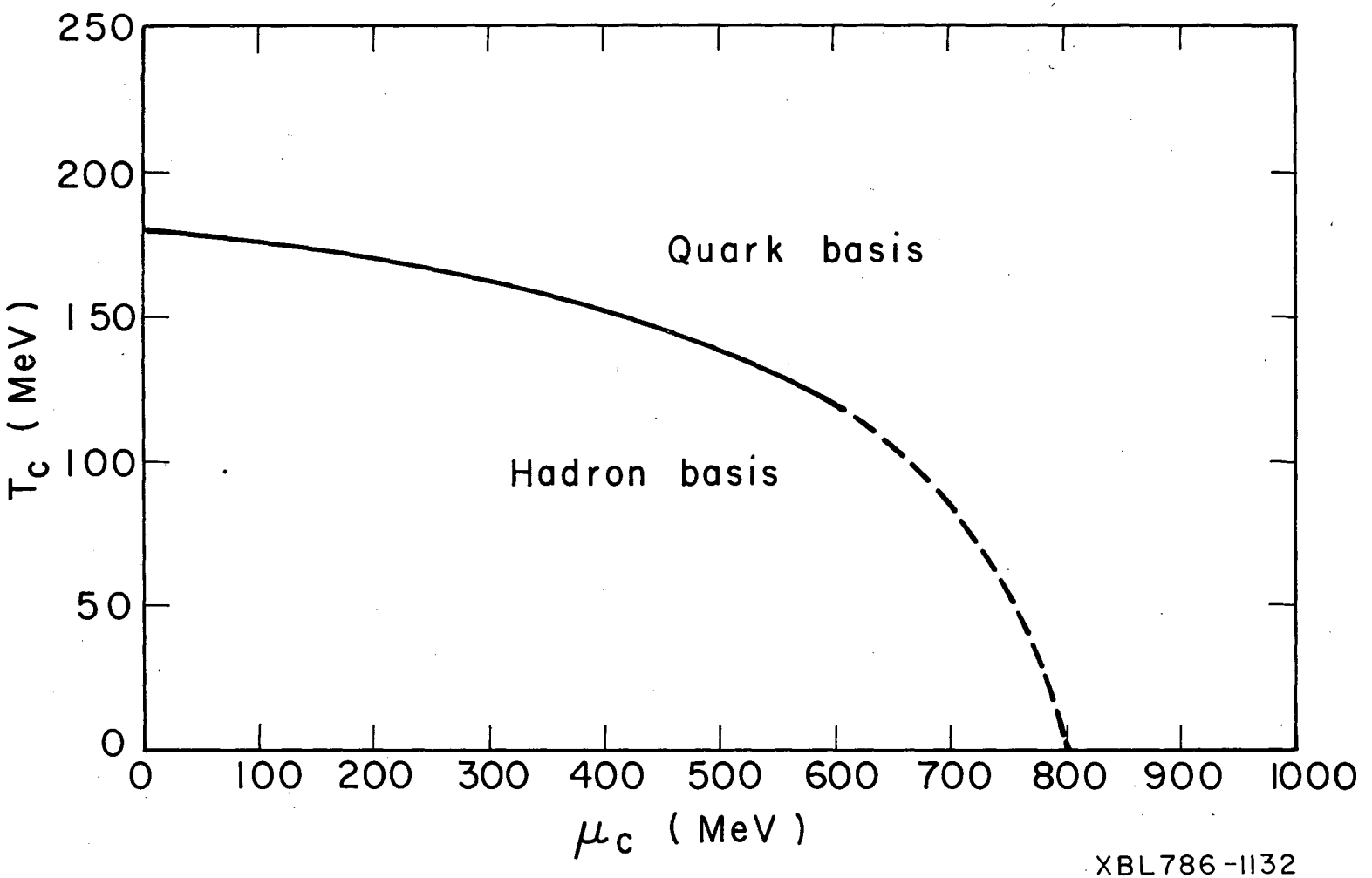
250
200
150
100
50
0
T_c (MeV)
Quark basis
Hadron basis
0
100
200
300
400
500
600
700
800
900
1000
μ_c (MeV)
XBL786-1132

Fig. 11

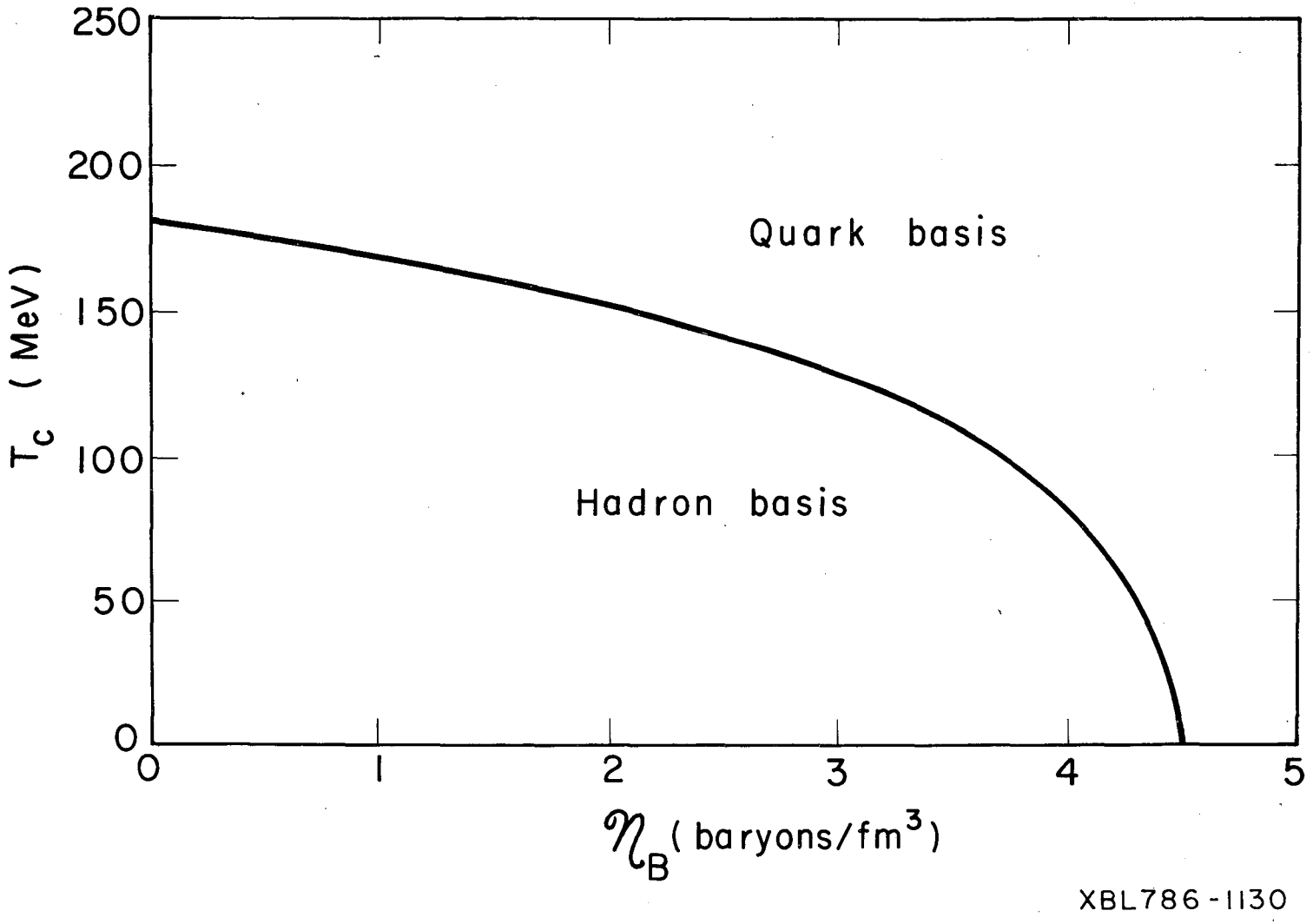
250
200
150
100
50
0
T_c (MeV)
Quark basis
Hadron basis
0
1
2
3
4
5
η_B (baryons/fm^3)
XBL786-1130

Fig. 12

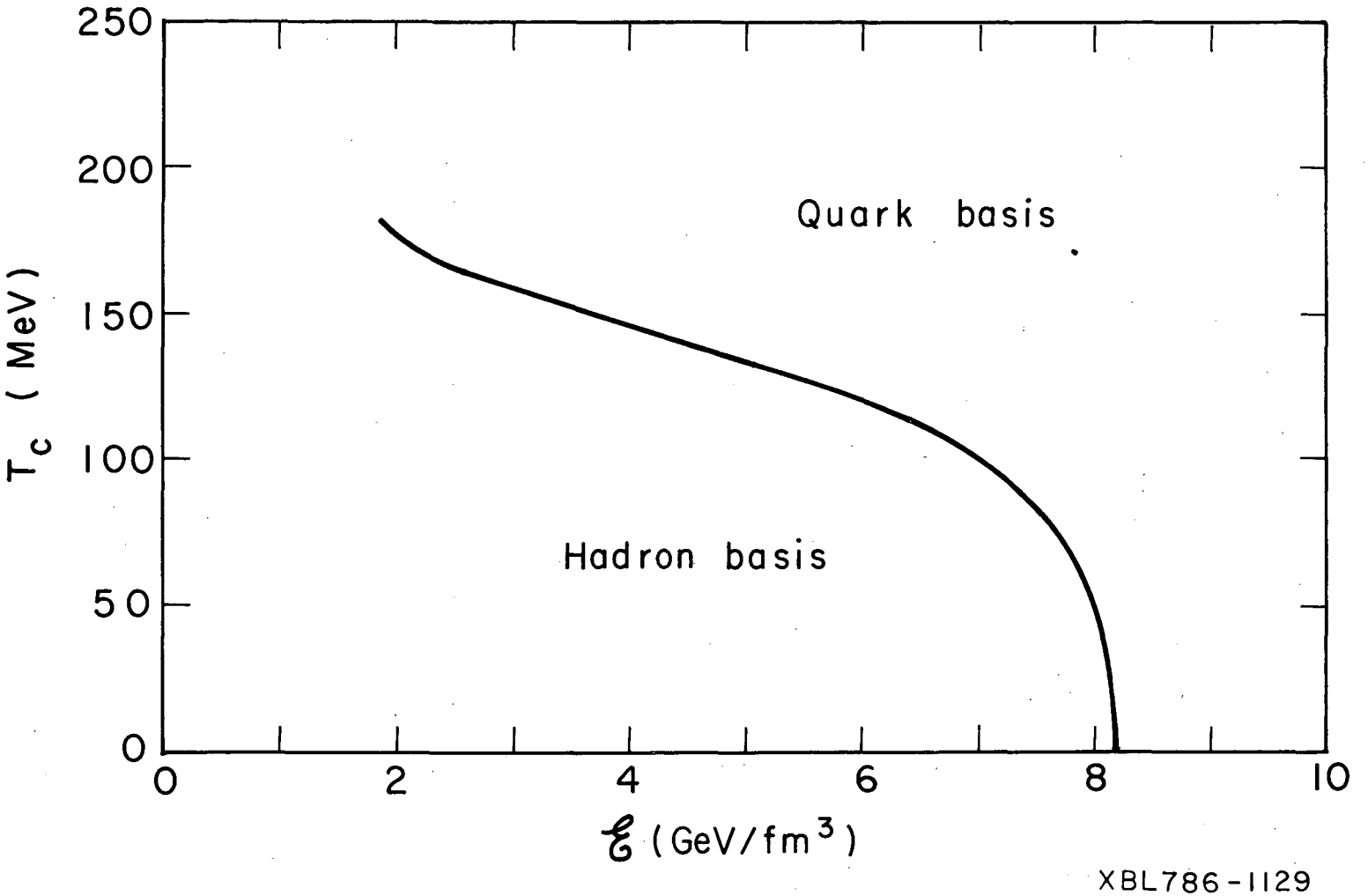
250
200
150
100
50
0
T_c (MeV)
Quark basis
Hadron basis
0
2
4
6
8
10
$\mathcal{E}$ (GeV/fm^3)
XBL786-1129

Fig. 13

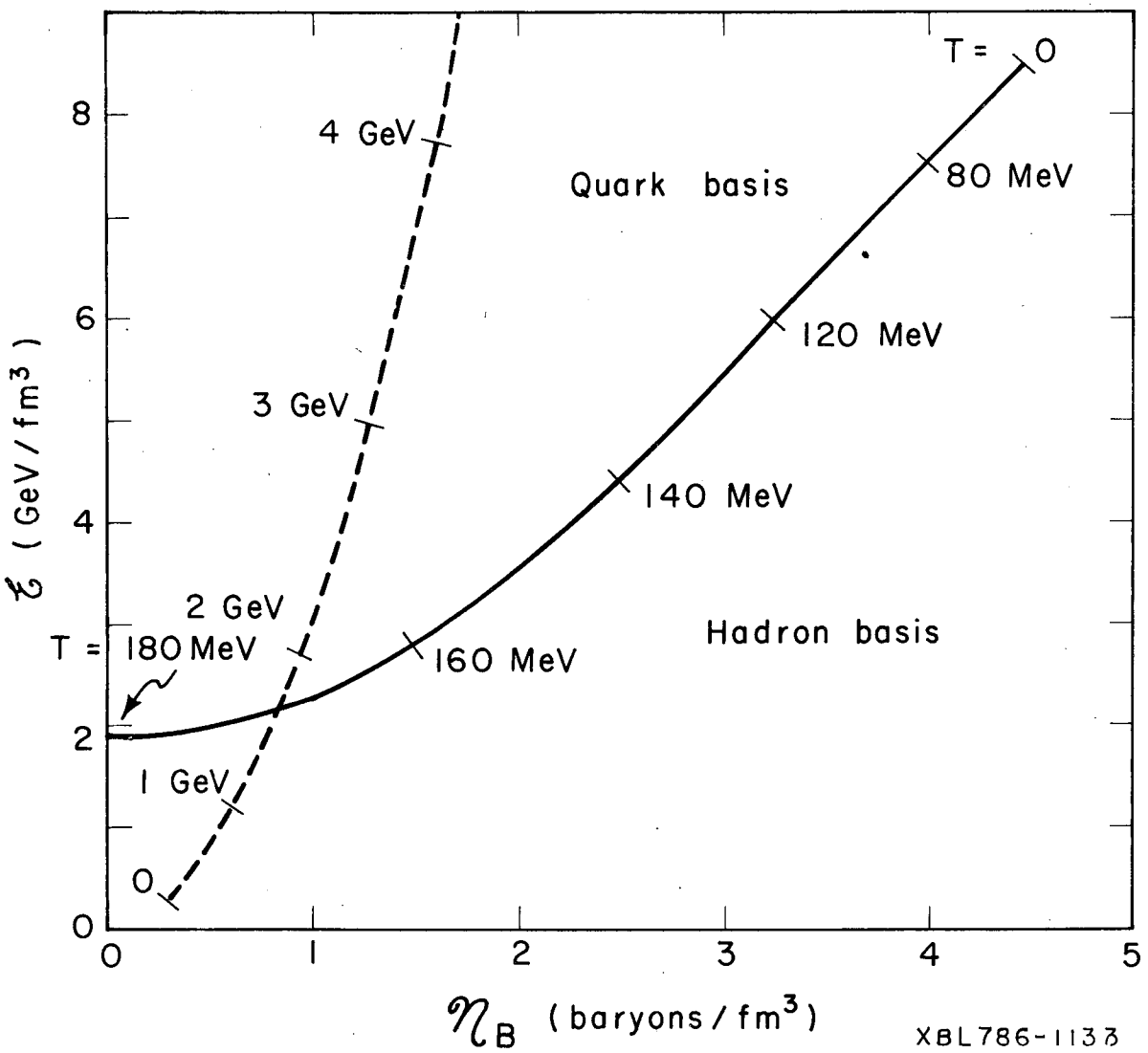
T = 0
80 MeV
120 MeV
140 MeV
160 MeV
180 MeV
T =
4 GeV
3 GeV
2 GeV
1 GeV
0
Quark basis
Hadron basis
ε (GeV/fm³)
η_B (baryons/fm³)
0
1
2
3
4
5
0
2
4
6
8
XBL786-1133

Fig. 14

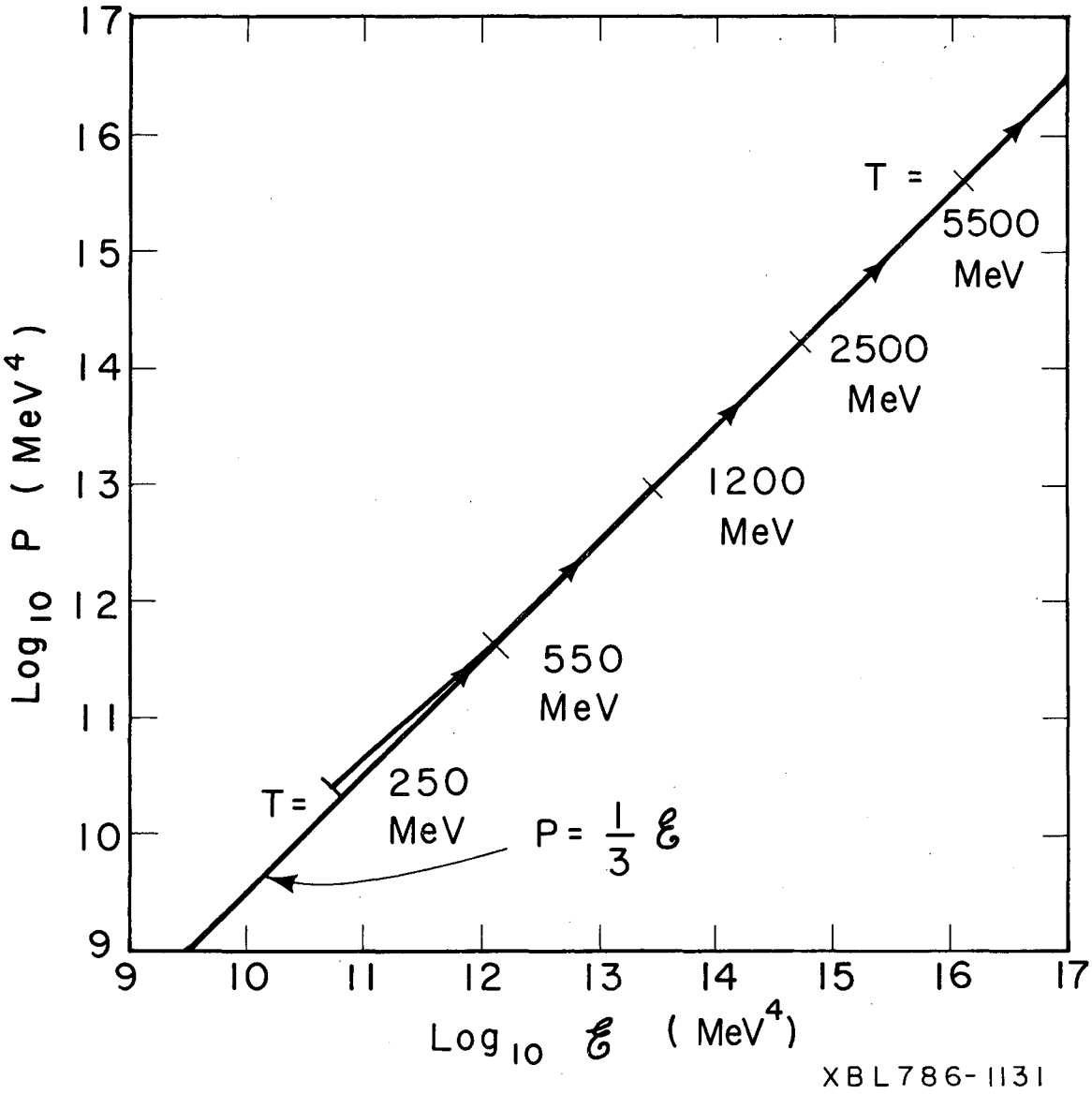
17
16
15
14
13
12
11
10
9
9
10
11
12
13
14
15
16
17
Log10 P (MeV4)
Log10 ℰ (MeV4)
T = 5500 MeV
2500 MeV
1200 MeV
550 MeV
T = 250 MeV
P = 1/3 ℰ
XBL786-1131

Fig. 15

This report was done with support from the Department of Energy. Any conclusions or opinions expressed in this report represent solely those of the author(s) and not necessarily those of The Regents of the University of California, the Lawrence Berkeley Laboratory or the Department of Energy.

TECHNICAL INFORMATION DEPARTMENT
LAWRENCE BERKELEY LABORATORY
UNIVERSITY OF CALIFORNIA
BERKELEY, CALIFORNIA 94720